Department of Justice, Office of Justice Programs, National Institute of Justice

Award Number: 2016-DN-BX-0169

The Utility of Multi-Dimensional Liquid Chromatography for the Analysis of Seized Drugs: Application to Emerging Drugs

Ira Saul Lurie

Research Professor

islurie@gwu.edu,

11/09/2017

The George Washington University

2121 Eye Street, NW, Washington D.C, 20052

Project Period 01/01/2017 to 12/31/2017

Final Summary Overview

The Utility of Multi-Dimensional Liquid Chromatography for the Analysis of Seized Drugs: Application to Emerging Drugs

Purpose of Project

The purpose of this project is to investigate whether multi-dimensional liquid chromatography can enhance the ability to identify emerging drugs. For this reason, the challenging separation of emerging drugs such as synthetic cannabinoids, bath salts, and phenethylamines, and certain of their positional isomers will be investigated.

The goal of this study is to establish multi-dimensional LC as a viable separation technique for the separation of seized drugs.

Project Design

Experiments were designed to answer the question whether multi-dimensional liquid chromatography can decrease the uncertainty of peak assignments of emerging drugs such as synthetic cannabinoids, synthetic cathinones and phenethylamines. In addition, the study was devised to ascertain the viability of multi-dimensional liquid chromatography for the analysis of seized drugs. The study consists of three phases. For the first phase, one dimensional (D1) separations were established for synthetic cannabinoids (Table 1), synthetic cathinones (Table 2), and phenethylamines (Table 3) in order to ascertain orthogonal separation conditions to employ for multi-dimensional separations. For the second phase, multi-dimensional separations were carried out for all three classes of emerging drugs using orthogonal separation conditions established in the first phase. These separations consisted of a D1 separation, heart cutting of peaks of interest onto a trapping loop, transfer to an appropriate trapping column (TC) and a complementary 2nd dimension (D2) separation.

Repeatability in both retention times and peak areas for both D1 and D2 separations was established, as well as the recovery of the peaks off the trapping column. The last phase is the analysis of simulated samples of synthetic cannabinoids, synthetic cathinones and phenethylamines employing the multi-dimensional chromatographic systems developed in the previous phases.

Methods

A Waters Acquity multi-dimensional UPLC system with two quaternary solvent systems (QSM), a binary solvent system (BSM), a column module (CM) containing two six port valves, a sample module (SM) containing a flow thru needle (FTN) fitted with a 15 µL loop, PDA-UV detector and a QDA MS detector is employed (Figure 1). For instrumental control and data handling Mass Lynx 4.1 is used.

For the D1 experiments, mixtures containing 21 controlled synthetic cannabinoids, JWH 018 and nine positional isomers, 16 controlled synthetic cathinones, ten sets of positional isomers of synthetic cathinones, 14 controlled phenethylamines, and 4 sets of positional isomers of phenethylamines were examined using various UHPLC columns (Table 4 particle size 1.7 µm and 1.8 µm) using either hydrophilic interaction chromatography (HILIC) and/or reversed phase chromatography (RPC). For the reversed phase chromatographic (RPC) separations ten minute gradients (with one minute hold) were for the most part performed using an acetonitrile modifier with a pH 2.3 formic acid additive, so that the controlled substances eluted from the beginning (approximately two times the void volume) and the end of the gradient space. A C8 column with methanol modifier with either a pH 2.3 formic acid additive and/ or an ammonium bicarbonate pH 11.6 buffer were also utilized for synthetic cathinones and phenethylamines. For HILIC (synthetic cathinones and phenethylamines) an

identical isocratic mobile phase containing 95% acetonitrile and 5% water with 5mM ammonium formate additive (prepared from a 200 mM buffer at pH 3.0) was used. All solutes eluted within 4 minutes. For synthetic cannabinoids, standard solutions were prepared from 100 µg/mL, 1 mg/mL, 5mg/mL or 10 mg/mL stock solutions and diluted to 5 µg/mL with methanol, followed by 1 µL injections. For synthetic cathinones and phenethylamines, standard solutions were prepared from 1 mg/mL stock solutions and diluted to 5 µg/mL with 0.5% formic acid in water, followed by 2.5 µL injections.

In order to evaluate the best combinations of separation columns to use for multidimensional separations the Neue selectively factor (S^2) as given by

$$S^2 = 1 - R^2 \qquad (1)^{[1]}$$

was used, where R^2 is the correlation coefficient of the retention time for column 1 versus column 2. Therefore, the higher the value of S^2 the more orthogonal is the use of two columns for multi-dimensional chromatography. Peak capacity n_c which measures the number of peaks that can be resolved in a chromatographic separation is an important parameter in measuring the separation power of a chromatographic system. For a resolution of 1, n_c can be defined by

$$n_c = (t_f - t_i) \div w_{av} \qquad (2)$$

where t_f is the time of the end of the final peak in the chromatogram, t_i is the time at the beginning of the first peak in the chromatogram and w_{av} is the average peak width at 0.67 base. For a separation the theoretical multi-dimensional peak capacity ${}^{2D}[n_c]_{theory}$ can be expressed by

$${}^{2D}[n_c]_{theory} = {}^{1}n_c * {}^{2}n_c \qquad (3)$$

where ${}^{1}n_c$ peak capacity of the first dimension and ${}^{2}n_c$ is the peak capacity of the 2nd separation dimension. Equation 3 assumes full coverage of the possible separation space, which is difficult to obtain in practice. The actual separation space utilized can be approximated by S^2 (the more orthogonal the separations the more separation space is utilized), and thus the actual multi-dimensional peak capacity ${}^{2D}[n_c]_{actual}$ can be estimated by

$$ {}^{2D}[n_c]_{actual} = {}^{1}n_c\left[1 + S^2\left({}^{2}n_c - 1\right)\right] \qquad (4) $$

whereby $\left[1 + S^2\left({}^{2}n_c - 1\right)\right]$ is the gain factor (estimated increase in peak capacity) in going from a D1 separation to a multi-dimensional separation. The peak capacity can also be a measure of uncertainly of peak assignments, since this term represents the number of possible unique retention times for a given chromatographic run.

Multi-dimensional separations were carried out with at column dilution (Figure 2, Figure 3) using a 150 µL loop, with 2% formic acid in water as loader and dilutor (1:20) for an XBridge BEH C18 trapping column (Table 4 particle size 10 µm), and 0.025% formic acid in acetonitrile as loader and dilutor (1:20) for an XBridge BEH HILIC trapping column (Table 4 particle size 10 µm). For % recovery experiments (D1 →D2), theoretical recovery values were obtained using D1 columns with MS detection, taking into account effects of flow rate and mobile phase conditions on peak areas.

For the synthetic cathinones and phenethylamines, 10 simulated samples each containing various adulterants and diluents were analyzed using multi-dimensional chromatography (Table 5, Table 6). Simulated cathinone and phenethylamine samples were prepared by pipetting appropriate amounts from 1 mg/mL methanol stock solutions of emerging drug(s) and adulterant or diluent, and diluting with 0.5% formic acid in water to a concentration of 5

µg/mL (synthetic cathinone or phenethylamine). 2.5 µL injections were employed. For the synthetic cannabinoids, 10 simulated samples containing various plant materials were analyzed using multi-dimensional chromatography (Table 7). Synthetic cannabinoid samples were prepared by pipetting appropriate amounts from 100 µg/mL- 10 mg/mL methanol or acetonitrile stock solutions and diluting with methanol to a concentration of 5 µg/mL (synthetic cannabinoid). 1.0 µL injections were employed. Standards were prepared by pipetting appropriate amounts of 100 µg/mL- 10 mg/ mL methanol or acetonitrile stock solutions and diluting with 0.5% formic acid in water or methanol to a concentration of 5 µg/mL (emerging drug, adulterant, diluent or plant material) for multi-dimensional analysis. 1.0 µL or 2.5 µL injections were employed for synthetic cannabinoid analysis, and synthetic cathinone and phenethylamine analysis, respectively.

Data Analysis

Various combinations of columns and mobile phases were investigated for the separation of emerging drugs in order to ascertain the best D1 and D2 conditions to utilize for multi-dimensional separations. Taking into account the charge state of the solute, peak capacity of the first dimension, the S^2 values, the gain factors, and the ability to standardize as much as possible the choice of the D1 and D2 columns, a C8 column was chosen for the first dimension while the bi-modal PFP column (ability to operate in the RPC and HILIC mode (2)) was chosen for the 2^{nd} dimension. Synthetic cannabinoids are primarily neutral compounds (JWH-200 tertiary amine), while synthetic cathinones are secondary and tertiary amines, and phenethylamines are primary and secondary amines. Due to their charge states, the synthetic cannabinoids are only amenable to RPC, while synthetic cathinones and phenethylamines are amenable to both RPC and HILIC. The first dimension should provide

relatively high peak capacity in order to provide a good overall separation of mixtures of controlled drugs of a given class for screening and confirmation purposes. In this vein, any column operating in the RPC mode would qualify. The BEH C8 column provided in combination with an HSS PFP column relatively high S^2values (≥0.5) for separations of controlled substances and well as positional isomers (Table 8). D1 separations for the controlled synthetic cannabinoids and the JWH-018 positional isomers employing a BEH C8 column and an HSS PFP column operating in the RPC mode, as well as the corresponding regression plots, are shown in Figure 4-Figure 9. Next D1 separations for the controlled synthetic cathinones and the pentedrone positional isomers employing a BEH C8 column operating in the RPC mode and an HSS PFP column operating in the HILIC mode, as well as the corresponding regression plots, are shown in Figure 10-Figure 15. Finally D1 separations for the controlled phenethylamines and the 25I-NBOMe positional isomers employing a BEH C8 column operating in the RPC mode and an HSS PFP column operating in the HILIC mode, as well as the corresponding regression plots, are shown in Figure 16-Figure 21.

Multi-dimensional separation parameters (${}^{1}n_c$, ${}^{2}n_c$, ${}^{2D}[n_c]_{theory}$, S^2, gain factor, and ${}^{2D}[n_c]_{actual}$) for the various separation conditions shown in Figure 4-Figure 21 are shown in Table 8. For the mixture of controlled synthetic cannabinoids, the peak capacity increases from 69 for a single dimension separation to an actual multi-dimensional peak capacity of 3352, therefore uncertainly of peak assignment decreases by approximately 50X using the latter chromatographic conditions. Lower gain factors of 13X and 4X, and lower actual multi-dimensional peak capacities of 662 and 270 were obtained for the mixture of controlled synthetic cathinones and controlled synthetic phenethylamines, respectively. The lower values for gain factors and multi-dimensional peak capacities for the latter emerging

drugs is due to the use of the relatively low peak capacities obtained when using HILIC for the second separation dimension. For the mixtures of positional isomers there are smaller increases in gain factors compared to which is obtained for the separations for a mixture of controlled substances (gain factors of 10, 10, 3 for JWH-018 isomers, pentedrone isomers, and phenethylamine 25I isomers, respectively). In addition, lower actual multi-dimensional peak capacities of 53, 88, and 14 was obtained for JWH-018 isomers, pentedrone isomers, and phenethylamine 25I isomers, respectively. For positional isomers the smaller values for gain factors and actual multi-dimensional peak capacities is due the relatively low peak capacities of both dimensions, due to the relatively narrow retention window in which positional isomers elute (t(f)- t(i)). In practice, for a larger subset of positional isomers an expanded retention window would exist, giving rise to larger gain factors and actual multi-dimensional peak capacities. As an alternative to HILIC, the use of a reverse phase column (BEH C8) with a high pH mobile phase was investigated as a second dimension for the synthetic cathinones and phenethylamines. Poor peak shapes were obtained for phenethylamines. For synthetic cathinones similar gain factors and multi-dimensional peak capacities are obtained when using either RPC with high pH or HILIC in the 2nd dimension. This arises due to the lower S^2 values obtained when using a C8 column with a high pH mobile phase for a D2 separation.

Multi-dimensional separations were carried out with at column dilution for select compounds for the systems described in Table 8 (Figure 22-Figure 35). For the hydrophobic synthetic cannabinoids an XBridge BEH C18 trapping column was used, while for the hydrophilic synthetic cathinones and phenethylamines an XBridge BEH HILIC trapping column was used. As shown in Figure 25 and Figure 26 for the D1 separation, JWH -250 and JWH-073

co-elute, as well as poor resolution for JWH-016 and JWH-018 2'-naphthyl-N-(1, 1-dimethylpropyl) isomer. However, for the D2 separation both pairs of solutes are well resolved, which illustrates the ability of multi-dimensional chromatography not only to significantly decrease the uncertainty of peak assignments based on retention time, but to allow more accurate quantitation (beyond the scope of this grant). Based on the significant gain factors in going from a D1 separation to a D2 separation, even fully resolved compounds in the first dimension should be subjected to a multi-dimensional separation. Since in most drug seizures only two or less emerging drugs would be present, this would limit the number of multi-dimensional runs required. Waters can now support a serial 9 heart cut loops from a single dimension separation, which means target peaks are stored in loop by their retention time order and release toward the trap and the 2^{nd} separation column in a serial mode.

For the various drug classes figures of merit were established for the multi-dimensional separations (Table 9). For this purpose, early, mid and late eluting compounds from the mixtures of controlled drugs or positional isomers were chosen as target compounds. Good retention time repeatability ($0.0 \geq \%RSD \geq 0.52$, $n = 5$), and for the most part good peak area repeatability ($0.44 \geq \%RSD \geq 9.6$, $n = 5$) were obtained for both the D1 and D2 separations.

Variable recoveries were obtained for transferring solutes from the D1 column, to the trapping loop, to the trapping column and subsequently to the D2 column ($1 \geq \%$ Recovery ≥ 135). A poor repeatability (%RSD peak area 37.7) was obtained for the D2 separation of AKB48 consistent with its poor recovery of 1%. However, excellent signal-to-noise (S/N) values were obtained for injections containing 5 µg/mL of each analyte ($924 \geq S/N \geq 75769$), rendering multi-dimensional chromatography suitable for routine analysis of seized drugs.

For ten simulated samples each of controlled synthetic cathinones, phenethylamines and synthetic cannabinoids (Table 5-Table 7) results for multi-dimensional chromatography are shown in Figure 36-Figure 38. For each of the target compounds in the presence of various adulterants, diluents or plant material contained in the individual sample, excellent D1 and D2 retention time matches are obtained for sample versus standard. For the various adulterants and diluents present in the simulated synthetic cathinone samples (Table 5), only lidocaine co-elutes in the D1 separation with any of the target solutes (α-PVP). As shown in Figure 39 for the D1 separation, the retention time of α-PVP is determined in the presence of lidocaine by the $[M+H]^+$ 218 trace which differs from the $[M+H]^+$ 235 trace for lidocaine. For the D2 separation lidocaine is now well separated from α-PVP. For the simulated sample containing 4-MePPP and pentedrone, the target solutes are partially resolved in the D1 separation and well resolved in the D2 separation (Figure 40). For the various adulterants present in the simulated phenethylamine samples (Table 6), only quinine co-elutes in the D1 separation with any of the target solutes (mescaline) (Figure 41). Again the retention time of the co-eluting solutes can be determined by the different $[M+H]^+$ traces. For the simulated sample containing 2C-T-2 and 2C-I the target solutes are significantly better resolved in the D2 separation than the D1 separation (Figure 42). None of the plant materials present in the simulated samples of synthetic cannabinoids interferes with the target solutes. For the simulated sample containing JWH-018 and JWH-081 a considerably improved separation is obtained for these solutes in the D2 separation versus the D1separation (Figure 43). JWH-019, RCS-8 and epi-CP47, 497 co-elute in the D1 separation but are well resolved in the D2 separation (Figure 44). A relatively weak response is obtained in the D2 separation for epi-

CP 47, 497 (sample 10) and CP 47, 497 (sample 3) with an approximate S/N = 20. The above examples again illustrate the excellent resolving power of multi-dimensional separations.

Scholarly Products Produced or in Process

Ochoa, C.M.; Schoenmakers, P.; Mallet, C.; Lurie, I.S.* Decreasing the uncertainty of peak assignments using multi-dimensional ultra-high performance liquid chromatography, manuscript in preparation.

Implications for Criminal Justice Policy and Practice in the United States

The use of multi-dimensional liquid chromatography would have a significant impact on the criminal justice system by increasing the likelihood of the correct identification of a seized drug by decreasing the uncertainty of peak identification during a chromatographic run. This is particularly useful for the identification of emerging drugs for which exists a wide range of similar drugs including analogs, homologs, positional isomers and diastereomers. Based on the above conclusions, multi-dimensional liquid chromatography would positively affect the backlog, by facilitating the screening and identification of emerging drugs. Instead of two separate chromatographic systems (e.g. GC and LC), orthogonal separations could be achieved in a single run. Although the technology for multi-dimensional liquid chromatography is commercially available (e.g. Waters and Agilent), very few, if any, forensic laboratories utilize this technology. The purpose of this project is to establish conditions which allow the routine use of this technology for case work. Toward this goal, the rational, feasibility of multi-dimensional liquid chromatography, and its applicability to real samples has been established.

Appendix

References

1. Neue, U.D.; O'Gara, J.E.; Mendez., A,. Selectivity in reversed-phase separations

Influence of the stationary phase, Journal of Chromatography A, 2006, 1127, 161-174.

2. Clyde, C.; Blake, S.; Obrien, S.; Igwilo, I.; Lurie, I.S. Application of mixed-mode ultra high performance liquid chromatography to forensic drug analysis, Analytical Methods, 2015 , 23, 9763-9772.

Table 1 UV and MS data for synthetic cannabinoids, including positional isomers

Solute	Structure	Formula Weight	UV Max	$[M+H]^+$
UR144	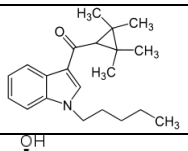	$C_{21}H_{29}NO$ 311.5	257.0 303.0	312.5
CP47,497	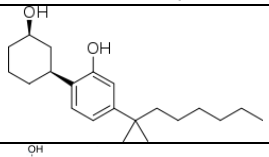	$C_{21}H_{34}O_2$ 318.5	275.0	301.2*
Epi CP 47, 497	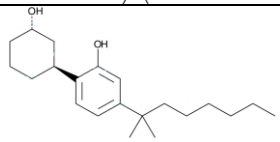	$C_{21}H_{34}O_2$ 318.5	275.0	301.3*
RCS4	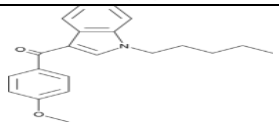	$C_{21}H_{23}NO_2$ 321.4	263.0 319.0	322.2
JWH-073	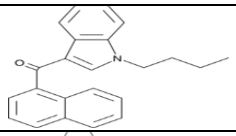	$C_{23}H_{21}NO$ 327.4	314.0	328.2
XLR-11	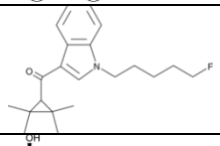	$C_{21}H_{28}FNO$ 329.2	255.7 302.7	330.3
CP47, 497 C8 homologue	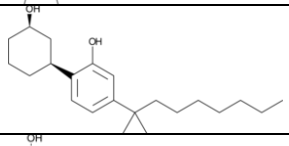	$C_{22}H_{36}O_2$ 332.5	275.0	315.5
3-epi CP47, 497 C8 homologue	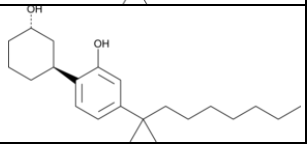	$C_{22}H_{36}O_2$ 332.5	275.0	315.2

JWH-250	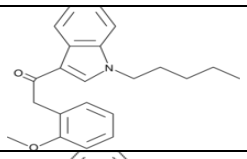	$C_{22}H_{25}NO_2$ 335.2	254.0 303.0	336.2
JWH-203	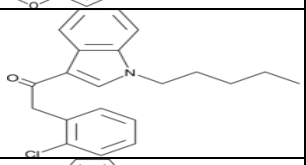	$C_{21}H_{22}ClNO$ 339.9	252.7 302.7	340.1
JWH-018	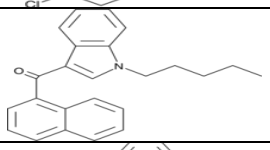	$C_{24}H_{23}NO$ 341.5	314.0	342.2
JWH-016	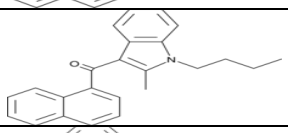	$C_{24}H_{23}NO$ 341.5	319.0	342.3
JWH-018 2'-naphthyl isomer	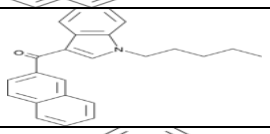	$C_{24}H_{23}NO$ 341.5	255.0 322.0	342.1
JWH-018 2'-naphthyl-N-(1, 1-dimethylpropyl) isomer	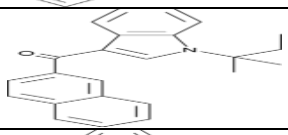	$C_{24}H_{23}NO$ 341.5	253.0 322.0	342.2
JWH-018 2'-naphthyl-N-(1, 2-dimethylpropyl) isomer	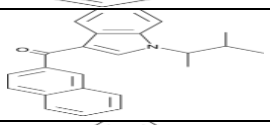	$C_{24}H_{23}NO$ 341.5	253.0 323.0	342.3
JWH-018 2'-naphthyl-N-(2, 2-dimethylpropyl) isomer	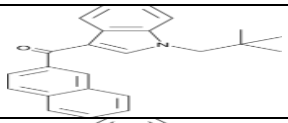	$C_{24}H_{23}NO$ 341.5	253.0 324.0	342.3
JWH-018 2'-naphthyl-N-(1 ethylpropyl) isomer	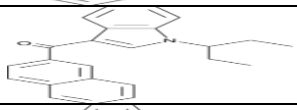	$C_{24}H_{23}NO$ 341.5	253.0 323.0	342.2
JWH-018 2'-naphthyl-N-(1 methylbutyl) isomer	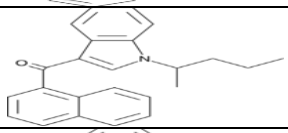	$C_{24}H_{23}NO$ 341.5	253.0 324.0	342.3
JWH-018 2'-naphthyl-N-(2methylbutyl) isomer	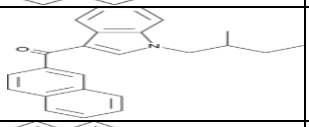	$C_{24}H_{23}NO$ 341.5	253.0 323.0	342.5
JWH-018 2'-naphthyl-N-(3 methylbutyl) isomer	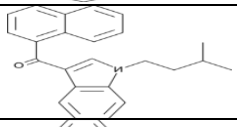	$C_{24}H_{23}NO$ 341.5	253.0 323.0	342.2
JWH-019	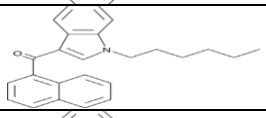	$C_{25}H_{25}NO$ 355.5	314.0	356.2
JWH-122	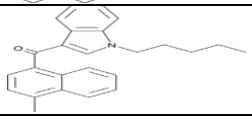	$C_{25}H_{25}NO$ 355.5	315.0	356.3

PB-22	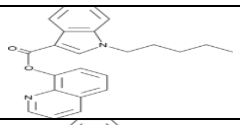	$C_{23}H_{22}N_2O_2$ 358.4	294.0	359.3
AM2201	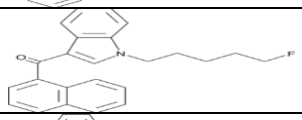	$C_{24}H_{22}FNO$ 359.4	314.0	360.2
AKB48	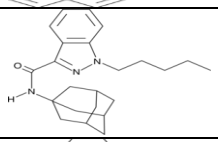	$C_{23}H_{31}N_3O$ 365.5	302.0	366.3
AB-Fubinaca	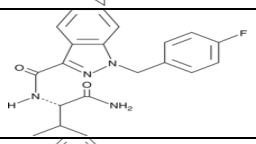	$C_{20}H_{21}FN_4O_2$ 368.4	301.0	369.2
JWH-081	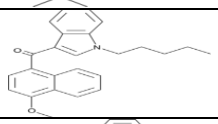	$C_{25}H_{25}NO_2$ 371.5	317.0	372.3
RCS8	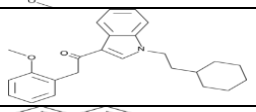	$C_{25}H_{29}NO_2$ 375.5	251.7 308.7	376.3
JWH-200	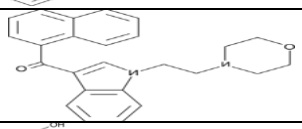	$C_{25}H_{24}N_2O_2$ 384.5	312.0	385.3
HU-210	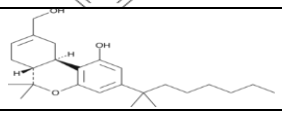	$C_{25}H_{38}O_3$ 386.6	281.0	387.3

*base peak

Table 2 UV and MS data for synthetic cathinones, including positional isomers

	Structure	Formula Weight	UV Max Low pH	UV Max HILIC	UV Max High pH	$[M+H]^+$
Cathinone	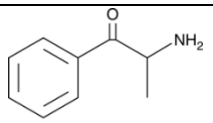	$C_9H_{11}NO$ 149.2	248.7	243.7	244.7	150.0
Methcathinone	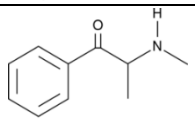	$C_{10}H_{13}NO$ 163.2	249.7	246.7	245.7	164.1
Nor-mephedrone	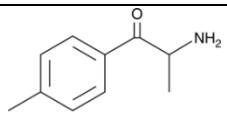	$C_{10}H_{13}NO$ 163.2	260.7	255.7	256.7	164.1
Mephredrone	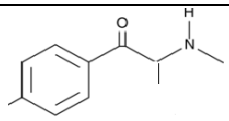	$C_{11}H_{15}NO$ 177.2	262.7	258.7	257.7	178.1
2-methylmethcathinone	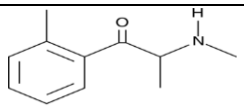	$C_{11}H_{15}NO$ 177.2	249.7 292.0	246.7 287.7	245.7 286.0	178.1
3-methylmethcathinone	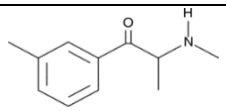	$C_{11}H_{15}NO$ 177.2	254.7	250.7 295.7	250.7 293.0	178.1
Buphedone	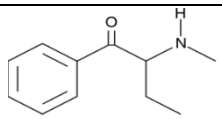	$C_{11}H_{15}NO$ 177.2	250.7	246.7	246.7	178.1
Ethcathinone	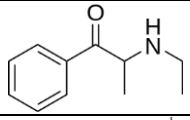	$C_{11}H_{15}NO$ 177.2	250.7	246.7	245.7	178.2
N.N-dimethylcathinone	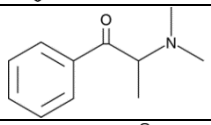	$C_{11}H_{15}NO$ 177.2	251.7	244.7	245.7	178.1
4-fluoromethcathinone	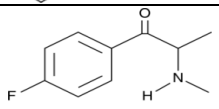	$C_{10}H_{12}FNO$ 181.2	252.7	248.7	247.7	182.2
3-fluoromethcathinone	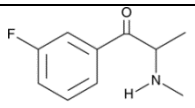	$C_{10}H_{12}FNO$ 181.2	246.7 290.7	242.7 286.7	242.7 285.7	182.1
Pentedrone	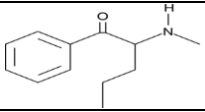	$C_{12}H_{17}NO$ 191.2	251.7	246.7	246.7	192.2
4-methylethcathinone	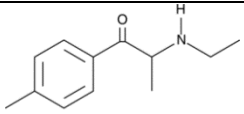	$C_{12}H_{17}NO$ 191.2	262.7	258.7	257.7	192.1

2,3-dimethylmethcathinone	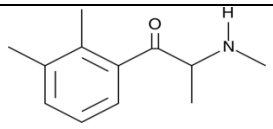	$C_{12}H_{17}NO$ 191.2	252.7	249.7	248.7	192.2
2,4-dimethylmethcathinone	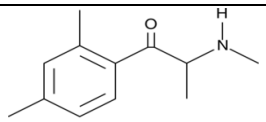	$C_{12}H_{17}NO$ 191.2	261.7	257.7	256.7	192.1
3,4-dimethylmethcathinone	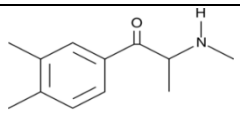	$C_{12}H_{17}NO$ 191.2	265.7	261.7	261.7	192.1
2-ethylmethcathione	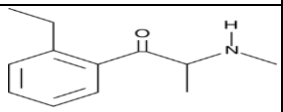	$C_{12}H_{17}NO$ 191.2	249.7 291.0	246.7 287.0	245.7 285.0	192.1
4-methylbuphedrone	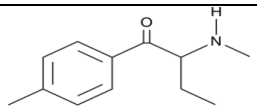	$C_{12}H_{17}NO$ 191.2	263.7	258.7	257.7	192.2
Methylone	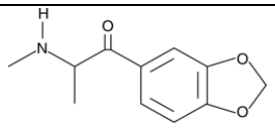	$C_{11}H_{13}NO_3$ 207.2	280.7 319.7	278.7 314.7	276.7 311.7	208.2
2,3-methylenedioxymeth-cathinone	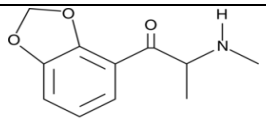	$C_{11}H_{13}NO_3$ 207.2	259.7 347.7	256.7 338.7	255.7 335.7	208.1
4-MePPP	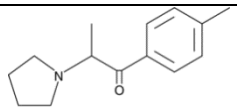	$C_{14}H_{19}NO$ 217.3	264.7	259.7	256.7	218.2
3-MePPP	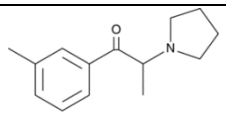	$C_{14}H_{19}NO$ 217.3	256.7 297.7	251.7 295.0	249.7 291.0	218.1
2-MePPP	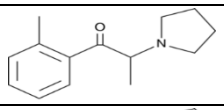	$C_{14}H_{19}NO$ 217.3	251.7 293.0	248.7 288.7	244.7 284.0	218.3
α-PBP	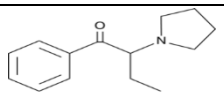	$C_{14}H_{19}NO$ 217.3	252.7	248.7	246.7	218.2
Butylone	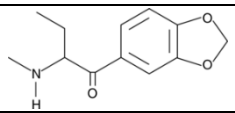	$C_{12}H_{15}NO_3$ 221.2	281.7 320.7	278.7 315.7	276.7 312.7	222.1
3,4-EDMC	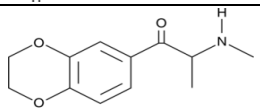	$C_{12}H_{15}NO_3$ 221.2	282.7 313.0	279.7 310.7	276.7 308.0	222.1
α-PVP	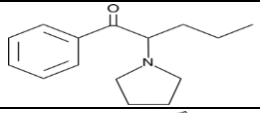	$C_{15}H_{21}NO$ 231.3	252.7	248.7	246.7	232.2
4-MePBP	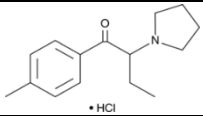	$C_{15}H_{21}NO$ 231.3	264.7	260.7	257.7	232.1

3-MePBP	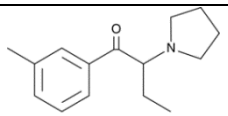	$C_{15}H_{21}NO$ 231.3	257.7 298.0	252.7 294.0	250.7 292.0	232.2
2-MePBP	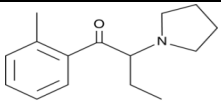	$C_{15}H_{21}NO$ 231.3	252.7 293.0	250.7 290.7	245.7 286.0	232.1
Pentylone	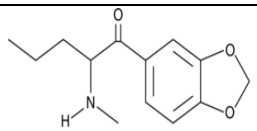	$C_{13}H_{17}NO_3$ 235.2	281.7 320.7	278.7 315.7	277.7 312.7	236.1
R-MMC	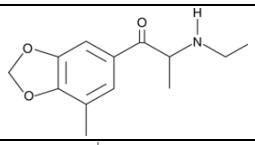	$C_{13}H_{17}NO_3$ 235.2	294.0 319.7	290.0 315.7	286.7 311.7	236.2
3,4-MDPV	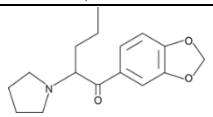	$C_{16}H_{21}NO_3$ 275.3	283.7 322.7	280.7 318.7	276.7 313.7	276.2
2,3-MDPV	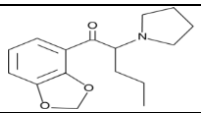	$C_{16}H_{21}NO_3$ 275.3	261.7 350.7	259.7 342.7	255.7 335.7	276.1
Naphyrone	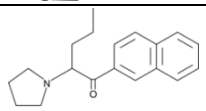	$C_{19}H_{23}NO$ 281.4	253.7 296.7 351.0	251.7 293.7 346.0	249.7 292.7 336.7	282.2

Table 3 UV and MS data for phenethylamines, including positional isomers

Solute	Structure	Formula Weight	UV Max	UV Max HILIC	$[M+H]^+$
2C-H	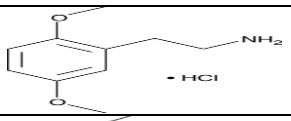	$C_{10}H_{15}NO_2$ 181.2	288.7	290.7	182.11
2C-D	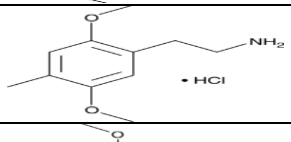	$C_{11}H_{17}NO_2$ 195.2	287.7	288.7	196.2
2C-E	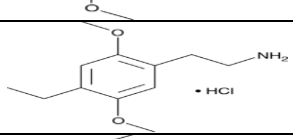	$C_{12}H_{19}NO_2$ 209.2	287.7	290.7	210.2
2C-G	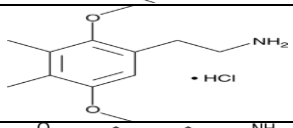	$C_{12}H_{19}NO_2$ 209.2	282.7	284.7	210.2
Mescaline	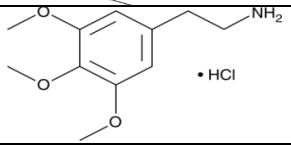	$C_{11}H_{17}NO_3$ 211.2	267.7	268.7	212.3
2C-C	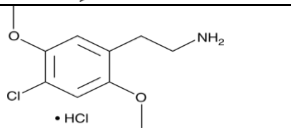	$C_{10}H_{14}CLNO_2$ 215.6	293.7	294.7	216.1
2C-P	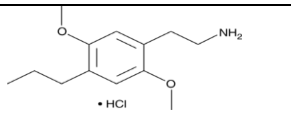	$C_{11}H_{15}NO$ 223.3	289.7	290.7	224.2
2C-N	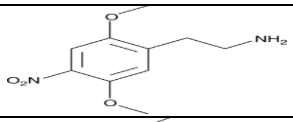	$C_{10}H_{14}N_2O_4$ 226.2	245.7 277.7 373.7	275.0 362.7	227.2
2C-T-2	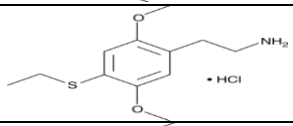	$C_{12}H_{19}NO_2S$ 241.3	251.7 302.7	252.7 304.7	242.3
2C-T-4	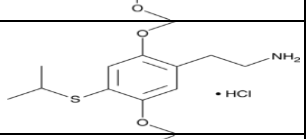	$C_{13}H_{21}NO_2S$ 255.3	252.7 302.7	253.7 304.7	256.1
2C-T-7	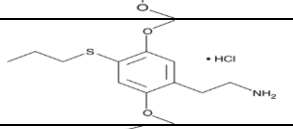	$C_{13}H_{21}NO_2S$ 255.3	251.7 302.7	252.7 304.7	256.3
2C-B	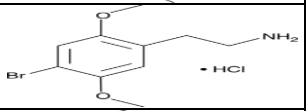	$C_{10}H_{14}BrNO_2$ 260.1	293.7	295.7	260.1
2C-I	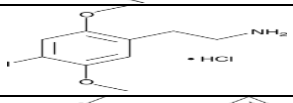	$C_{10}H_{14}INO_2$ 307.1	296.7	298.7	308.0
25E-NBOMe	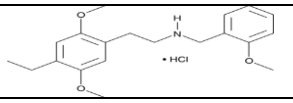	$C_{20}H_{27}NO_3$ 329.4	279.7	280.7	330.2

25G-NBOMe	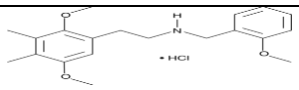	$C_{20}H_{27}NO_3$ 329.4	277.7	278.7	330.2
25C-NBOMe	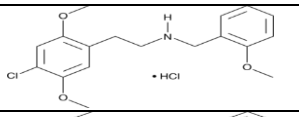	$C_{18}H_{22}ClNO_3$ 335.8	280.7 293.7	280.7 294.7	336.2
25B-NBOMe	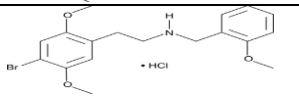	$C_{18}H_{22}BrNO_3$ 380.2	280.7 295.7	280.7 295.7	380.2
25I-NBOMe 4 methoxy isomer	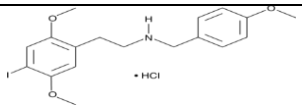	$C_{18}H_{22}INO_3$ 427.0	296.7	298.7	428.2
25I-NBOMe 3 methoxy isomer	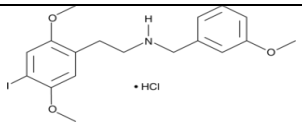	$C_{18}H_{22}INO_3$ 427.0	282.7 297.7	282.7 297.7	428.2
25I-NBOMe	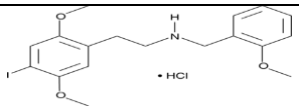	$C_{18}H_{22}INO_3$ 427.0	280.7 297.7	279.7 298.7	428.2

Table 4 UHPLC and trapping columns used in study

Chemistry	Particle Size (µm)	Dimensions	Pore Size (Å)	Carbon load (%)	Ligand Type	pH range
BEH C18	1.7	2.1 mm x 100	130	18	Trifunctional C18	1-12
BEH C8	1.7	2.1 mm x 100	130	13	Trifunctional C8	1-12
BEH Phenyl	1.7	2.1 mm x 100	130	15	Trifunctional Phenyl-Hexyl	1-12
BEH HILIC	1.7	2.1 mm x 50	130	unbonded	unbonded	1-9
HSS T3	1.8	2.1 mm x 100	100	11	Trifunctional C18	2-8
HSS PFP	1.8	2.1 mm x 100	100	7	Trifunctional Pentafluoro-phenyl	2-8
HSS PFP	1.8	2.1 mm x 50	100	7	Trifunctional Pentafluoro-phenyl	2-8
XBridge BEH C18 direct connect	10	2.1 mm x 30	130	18	Trifunctional C18	1-12
XBridge BEH C8 direct connect	10	2.1 mm x 30	130	13	Trifunctional C8	1-12
Oasis HLB direct connect	20	2.1 mm x 30	80		N-Vinylpyrrolidone-DVB copolymer	0-14
XBridge BEH HILIC direct connect	10	2.1 mm x 30	130		unbonded	1-9

ww.waters.com/waters/home.htm?locale=en_US

Table 5 Simulated synthetic cathinone samples

Sample #	emerging drug	concentration	adulterants	concentration
1	methcathinone	250 ug/mL	lidocaine	1mg/mL
2	butylone	100 ug/mL	caffeine	1mg/mL
3	3,4-MDPV	250 ug/mL	benzocaine	1mg/mL
4	naphyrone	100 ug/mL	pancake mix	1mg/mL
5	buphedrone	50 ug/mL	lidocaine	1mg/mL
6	Pentylone*	10 ug/mL	caffeine	1mg/mL
7	alpha-PBP	100 ug/mL	lidocaine	1mg/mL
8	pentedrone 4-MePPP	100 ug/mL each	caffeine	1mg/mL
9	4-fluoromethcathinone alpha- PVP	100 ug/mL each	benzocaine	1mg/mL
10	3-fluoromethcathinone mephedone 4-methylethcathinone	100 ug/mL each	benzocaine	1mg/mL

*inject 1 uL

Table 6 Simulated phenethylamine samples

Sample #	emerging drug	concentration	adulterants	concentration
1	2C-H	250 ug/mL	benzocaine	1mg/mL
2	2C-D	100 ug/mL	caffeine	1mg/mL
3	mescaline	250 ug/mL	quinine	1mg/mL
4	2C-E	100 ug/mL	tetracane	1mg/mL
5	2C-T-7	50 ug/mL	benzocaine	1mg/mL
6	2C-P*	10 ug/mL	caffeine	1mg/mL
7	25B-NBOMe	100 ug/mL	quinine	1mg/mL
8	2C-T-2 2C-I	100 ug/mL each	tetracaine	1mg/mL
9	2C-C 2C-T-4	100 ug/mL each	benzocaine	1mg/mL
10	2C-N 2C-B 25C-NBOMe	100 ug/mL each	caffeine	1mg/mL

*inject 1 uL

Table 7 Simulated synthetic cannabinoid samples

Sample #	emerging drug	concentration	adulterants	concentration
1	AB-Fubinaca	2.5 ug/mL	marshmallow leaf	1mg/mL
2	PB-22	10 ug/mL	dog rose leaf	1mg/mL
3	CP47, 497	50 ug/mL	beach bean leaf	1mg/mL
4	AKB 48	5 ug/mL	honey weed leaf	1mg/mL
5	JWH-2037	10 ug/mL	marshmallow leaf	1mg/mL
6	JWH-122	25 ug/mL	dog rose leaf	1mg/mL
7	HU-210	5 ug/mL	beach bean leaf	1mg/mL
8	RCS-4 JWH-019	25 ug/mL each	honey weed leaf	1mg/mL
9	JWH-018 JWH-081	10 ug/mL each	marshmallow leaf	1mg/mL
10	JWH-019 RCS-8 epi-CP47, 497	50 ug/mL each	dog rose leaf	1mg/mL

Table 8- Separation parameters for emerging drugs for select multi-dimensional separations

Solute	${}^{1}n_c$	${}^{2}n_c$	${}^{2D}[n_c]_{theory}$	S^2	Gain Factor	${}^{2D}[n_c]_{actual}$
Controlled Synthetic Cannabinoids	69 (C8)	54 (PFP_{RP})	3726	0.9068	49	3352
JWH-018 Positional Isomers	5 (C8)	20 (PFP_{RP})	100	0.4839	10	53
Controlled Synthetic Cathinones	51 (C8)	24 (PFP_{HILIC})	1224	0.5268	13	662
Pentedrone Positional Isomers	9 (C8)	11 (PFP_{HILIC})	99	0.8971	10	88
Controlled Synthetic Phenethyl-amines	62 (C8)	8 (PFP_{HILIC})	496	0.4642	4	270
Phenethyl-amine 25I Positional Isomers	5 (C8)	9 (PFP_{HILIC})	45	0.2289	3	14

Table 9- Figures of merit for multi-dimensional separations[a]

Solute 5 µg/mL	%RSD RT D1 n=5	%RSD RT D2 n=5	%RSD Peak Area D1 n=5	%RSD Peak Area D2 n=5	% Recovery	Average S/N n=5
AB-Fubinaca	0.00	0.06	7.7	1.5	135	12295
PB-22	0.07	0.06	0.29	8.7	91	29059
AKB48	0.04	0.12	0.29	37.7	1	924
methcathinone	0.21	0.27	0.44	3.0	33	15778
pentylone	0.15	0.12	4.8	2.8	52	53021
naphyrone	0.08	0.25	0.89	9.6	44	43271
2C-H	0.00	0.13	4.3	1.1	27	15997
2C-E	0.17	0.16	3.2	1.2	45	26134
25I-NBOMe	0.06	0.52	2.5	2.0	79	75769

[a] MS detection with selected ion response (SIR)

Figure 1- Multi-dimensional liquid chromatographic system employed in NIJ study

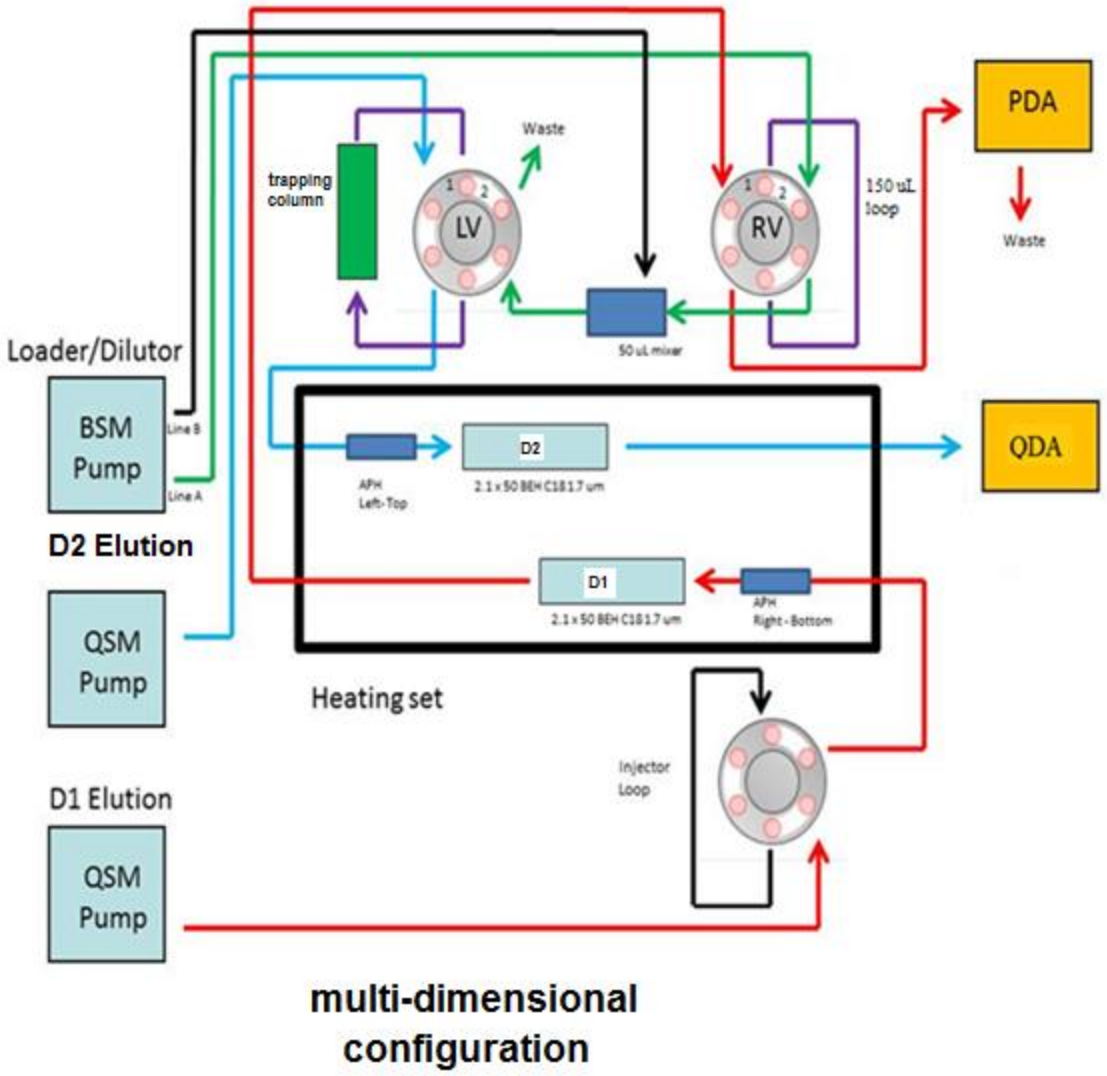

Figure 2- Schematic diagram for a multi-dimensional separation.

Using the supplied hardware there are five steps in carrying out a multi-dimensional LC separation, with time de-coupled chromatography and at-column dilution (see Figure 3).

The left valve (LV) and right valve (RV) can be in either position 1 or position 2.

Step 1: First dimension separation with PDA detection
Valves: Original position
Left Valve: Position 2 Right Valve: Position 2
QSM- D1 pump: First dimension separation begins using PDA detection
BSM: Flows through the parking loop and pre-treats the trap cartridge and flows to waste
QSM- D2 pump: Flow equilibrates D2 column, flows into QDA

Step 2: Heart-cut of the first dimension peak(s) of interest
Valves: Right valve switches in order to cut, or transfer, the peak from first dimension analysis

Left Valve: Position 2 Right Valve: Position 1
QSM- D1 pump: Drives the transfer to the parking loop
BSM: Still pre-treats the trap cartridge and flows to waste
QSM- D2 pump: Still running initial equilibration for the D2 column

Step 3: Transfer of heart-cut of the first dimension peak of interest from parking loop to trap cartridge
Valves: Right valve switches in order to transfer the peak from the parking loop to the trap cartridge
Left Valve: Position 2 Right Valve: Position 2
QSM- D1 pump: First dimension separation resumes
BSM: Drives the transfer from the parking loop to the trap cartridge while diluting the solvent strength of the heart cut in order to facilitate retention on the trap cartridge
QSM- D2 pump: Still running initial equilibration for the D2 column

Step 4: Back-flush and separation with QDA detection
Valves: Left valve switches to bring the QSM-D2 pump flow in line with the trap cartridge
Left Valve: Position 1 Right Valve: Position 2
QSM- D1 pump: separation continues until completed then re-equilibration occurs
BSM: flushes parking loop and flows to waste. Flow can be stopped or reduced at this point
QSM- D2 pump: Back-flushes the trap cartridge moving the transferred analyte(s) to the head of the D2 column and subsequent separation with QDA detection

Step 5: Return to initial conditions
Valves: Left valve switches back to the original position
Left Valve: Position 2
Right Valve: Position 2
QSM- D1 pump: Re-equilibration of D1 column
BSM: Flushing parking loop and trap cartridge and flows to waste
QSM- D2 pump: Re-equilibration of D2 column

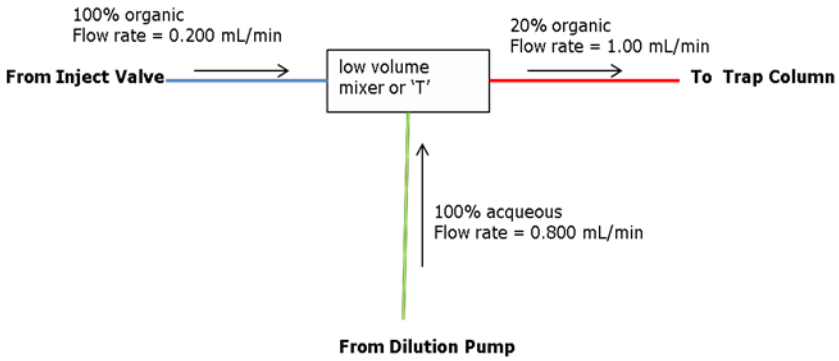

Figure 3- Schematic diagram for at-column dilution for a multi-dimensional separation.

Sample delivered with variable organic composition (dependent on composition contained in transferred volume)

Dilution flow 100% aqueous or high organic depending on trapping column

Ratio of flow rates determines degree of dilution

Required dilution will change with the hydrophobicity of the analyte(s) for RPC trapping column (rule of thumb- 20-30% decrease in organic composition to start, should facilitate retention). For HILIC trapping column acetonitrile concentration approaching 100% would be required to trap solutes based on hydrophilicity of the analyte.

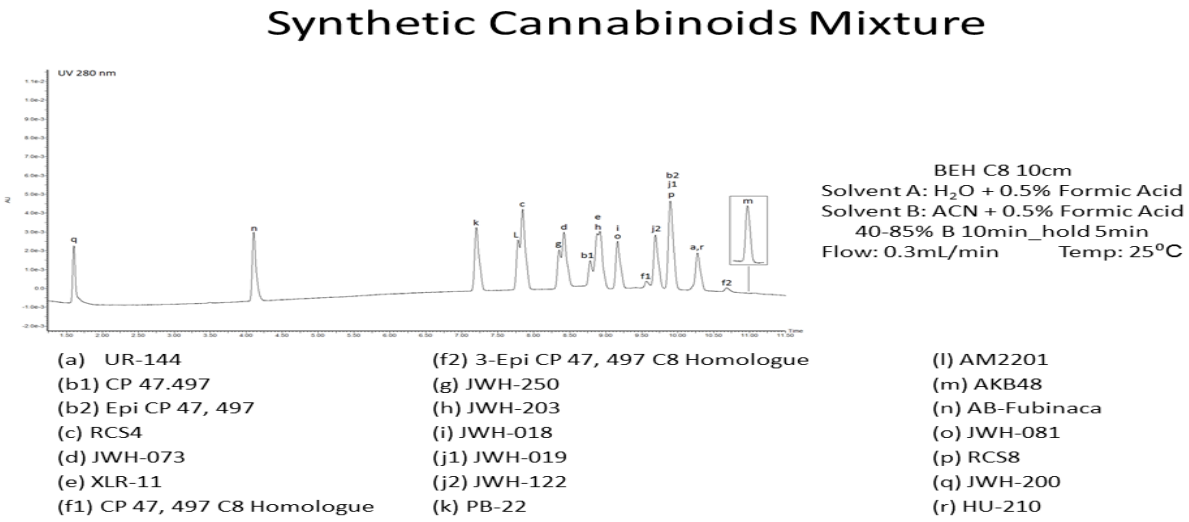

Figure 4- UHPLC separation of controlled synthetic cannabinoids employing a C8 column.

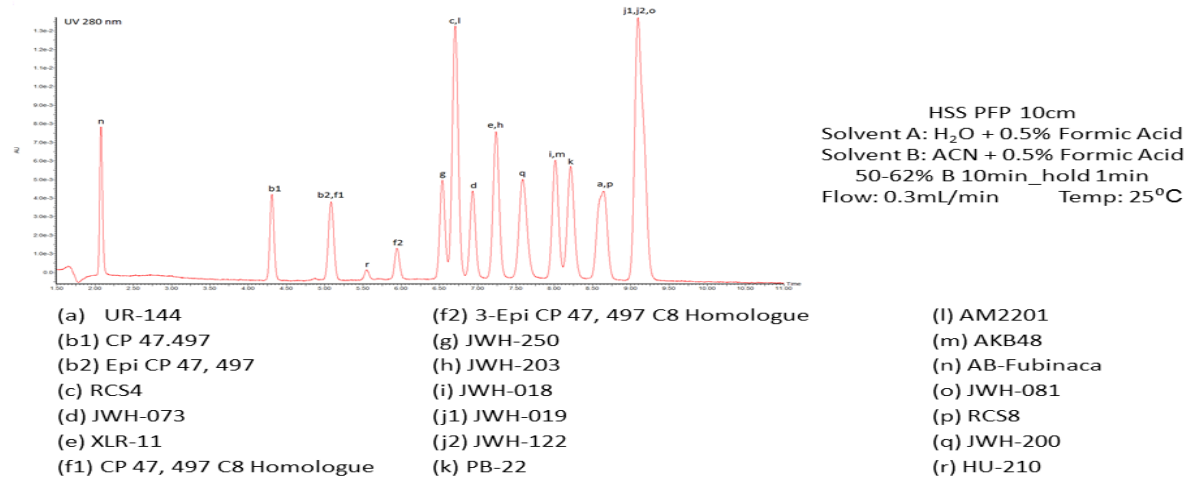

Figure 5- UHPLC separation of controlled synthetic cannabinoids employing a PFP column in the RPC mode.

This resource was prepared by the author(s) using Federal funds provided by the U.S. Department of Justice. Opinions or points of view expressed are those of the author(s) and do not necessarily reflect the official position or policies of the U.S. Department of Justice.

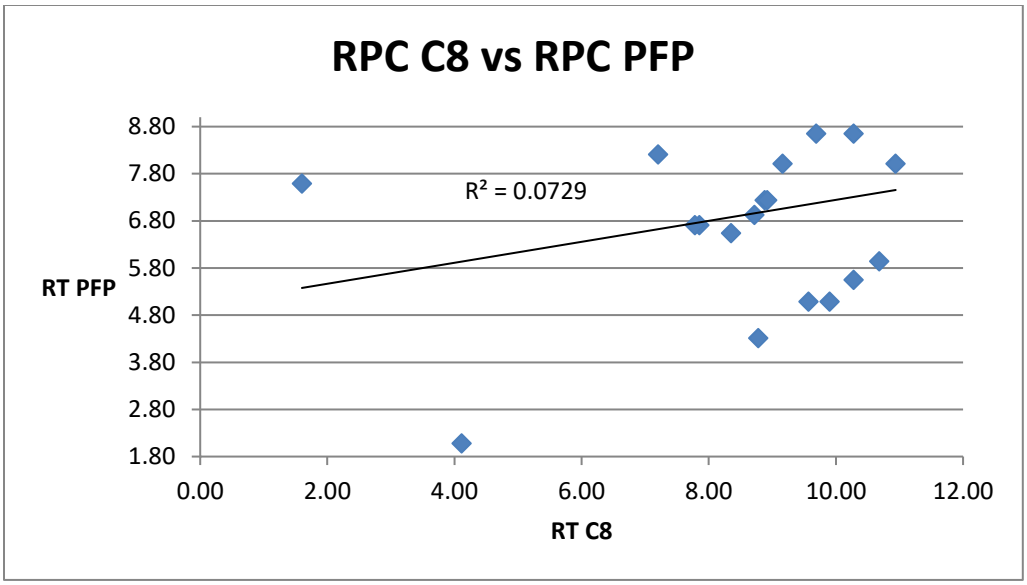

Figure 6- RT C8 versus RT PFP for a mixture of controlled synthetic cannabinoids.

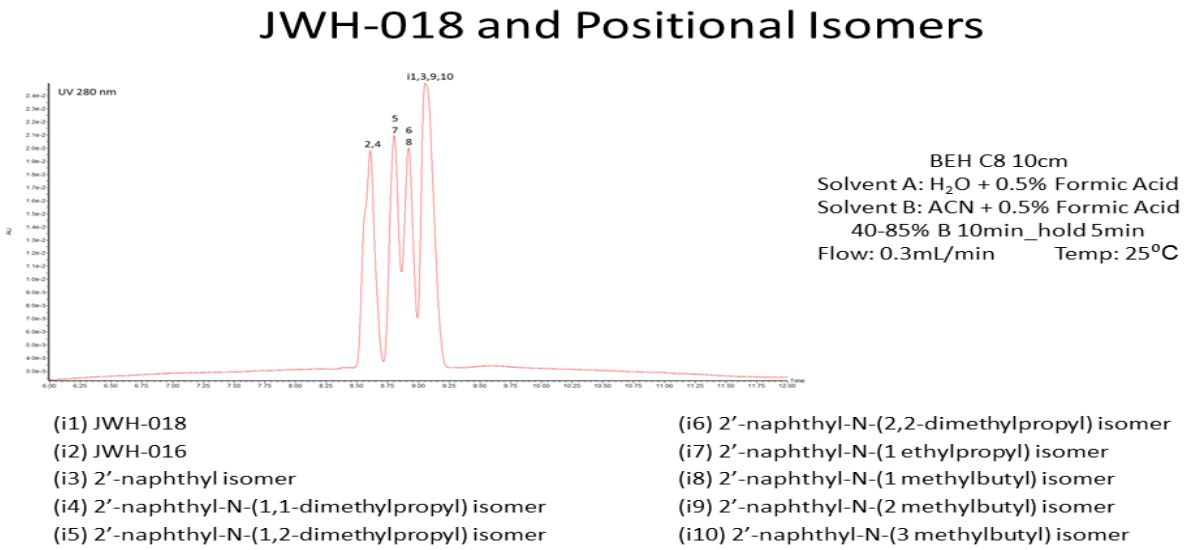

Figure 7- UHPLC separation of JWH-018 positional isomers employing a C8 column.

This resource was prepared by the author(s) using Federal funds provided by the U.S. Department of Justice. Opinions or points of view expressed are those of the author(s) and do not necessarily reflect the official position or policies of the U.S. Department of Justice.

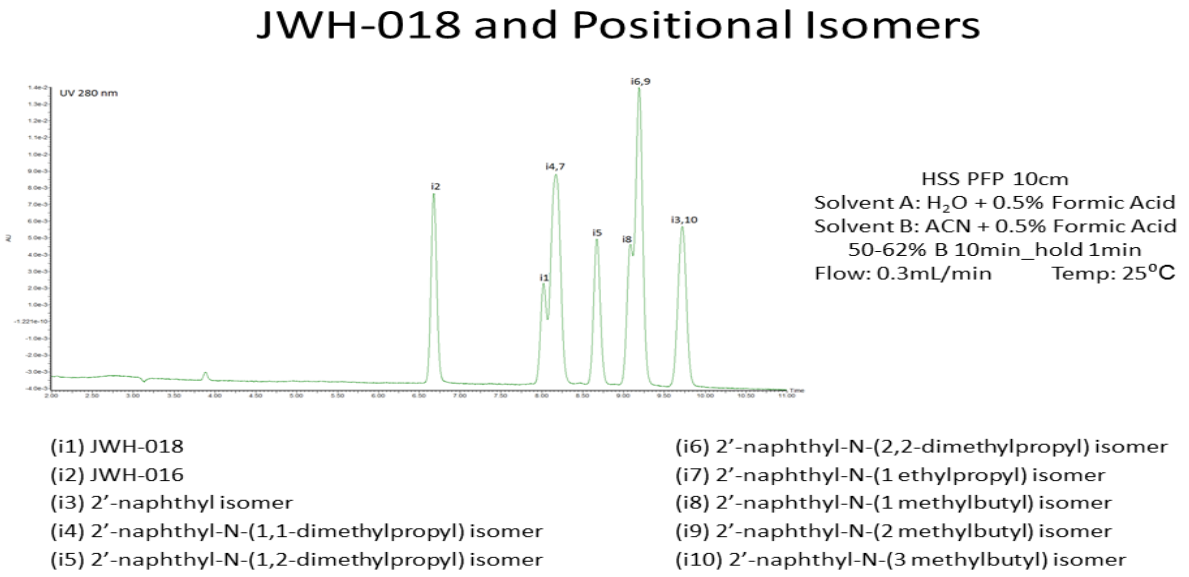

Figure 8- UHPLC separation of JWH-018 positional isomers employing a PFP column in the RPC mode.

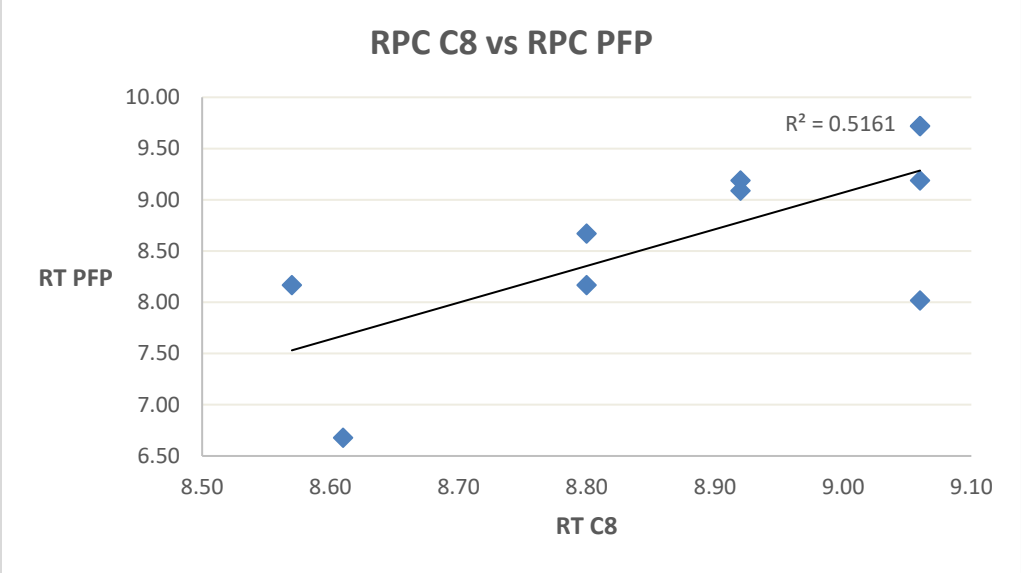

Figure 9- RT C8 versus RT PFP for a mixture of JWH 018 positional isomers.

This resource was prepared by the author(s) using Federal funds provided by the U.S. Department of Justice. Opinions or points of view expressed are those of the author(s) and do not necessarily reflect the official position or policies of the U.S. Department of Justice.

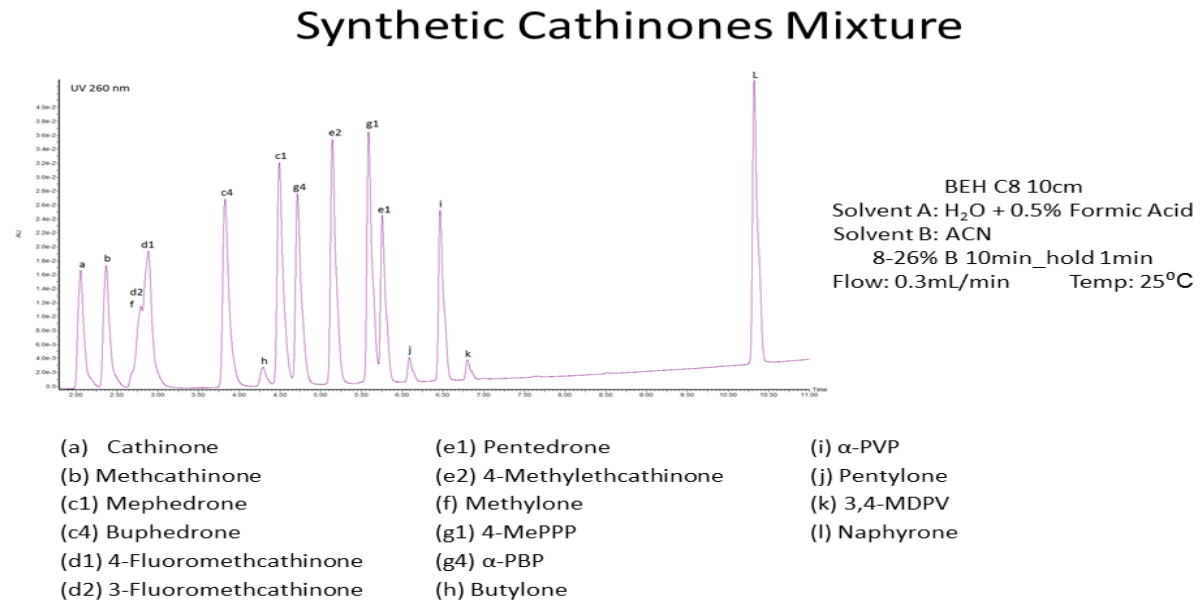

Figure 10- UHPLC separation of controlled synthetic cathinones employing a C8 column.

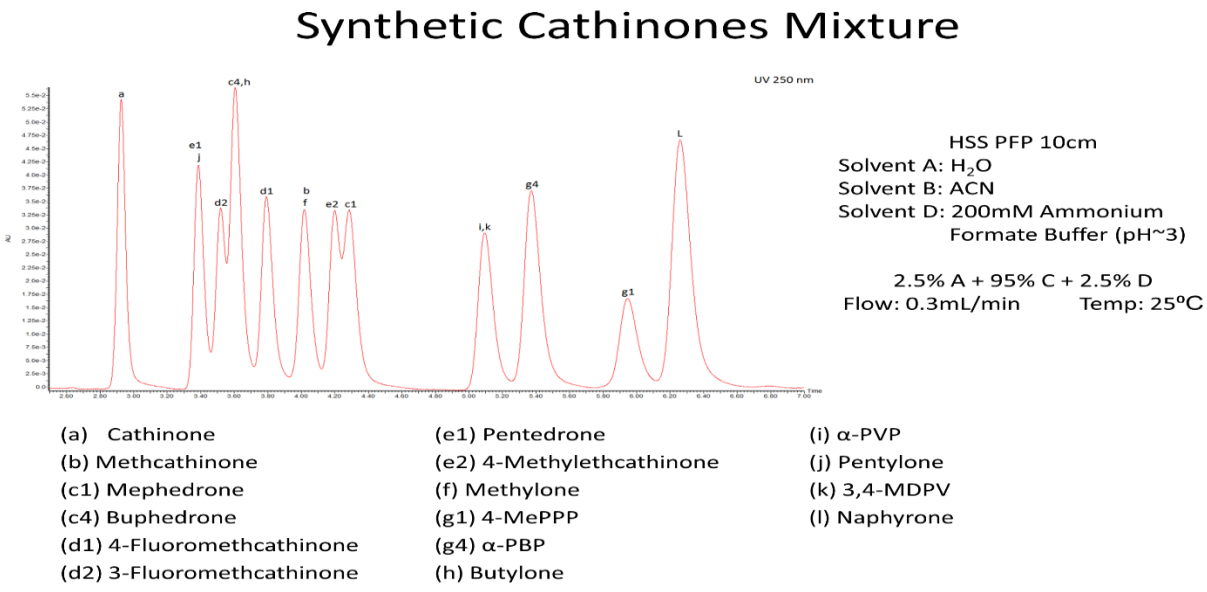

Figure 11- UHPLC separation of controlled synthetic cathinones employing a PFP column in the HILIC mode.

This resource was prepared by the author(s) using Federal funds provided by the U.S. Department of Justice. Opinions or points of view expressed are those of the author(s) and do not necessarily reflect the official position or policies of the U.S. Department of Justice.

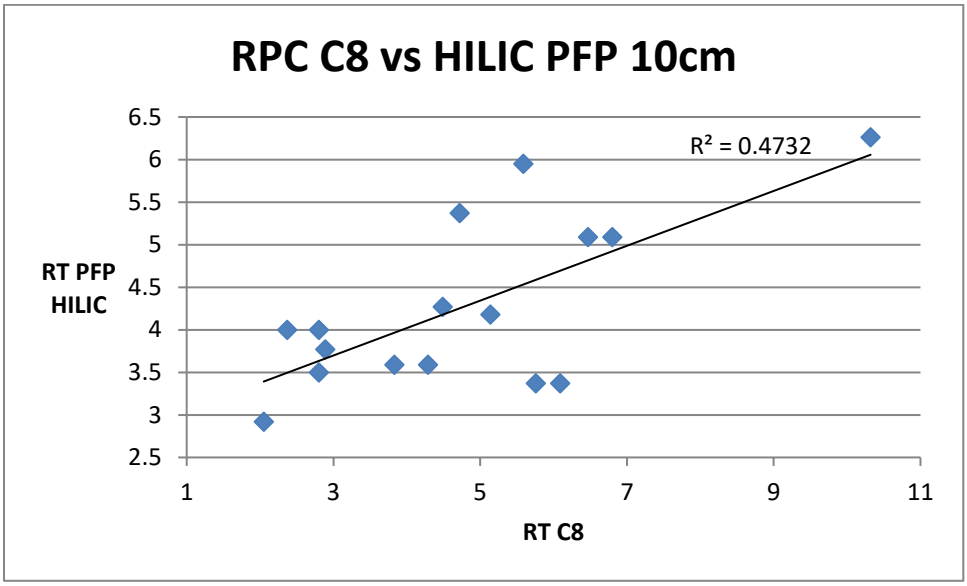

Figure 12- RT C8 versus RT PFP for a mixture of controlled synthetic cathinones.

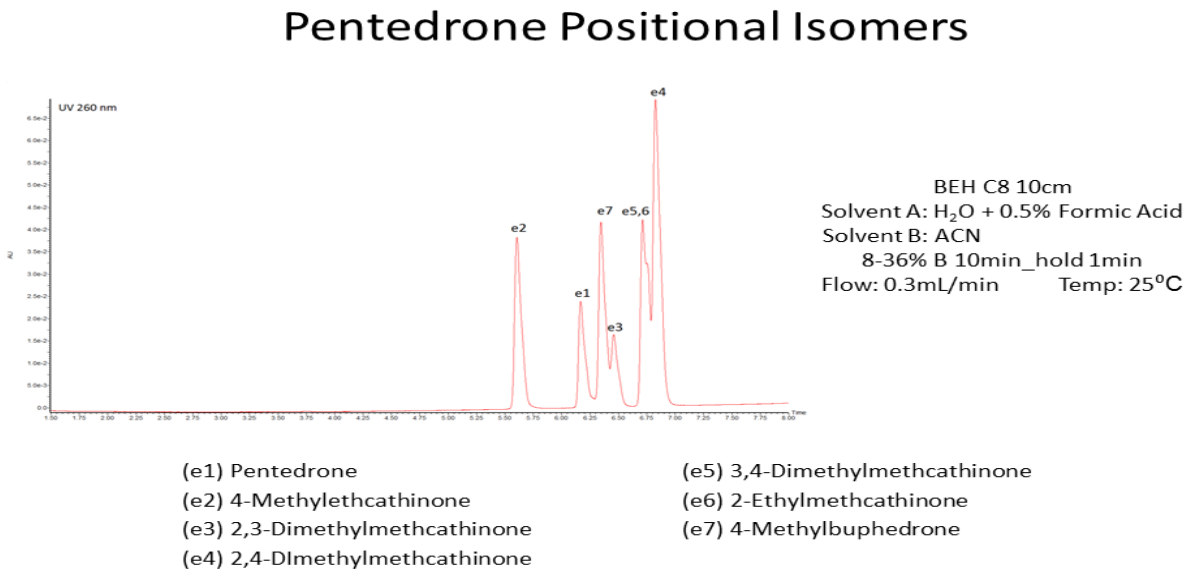

Figure 13- UHPLC separation of pentedrone positional isomers employing a C8 column.

This resource was prepared by the author(s) using Federal funds provided by the U.S. Department of Justice. Opinions or points of view expressed are those of the author(s) and do not necessarily reflect the official position or policies of the U.S. Department of Justice.

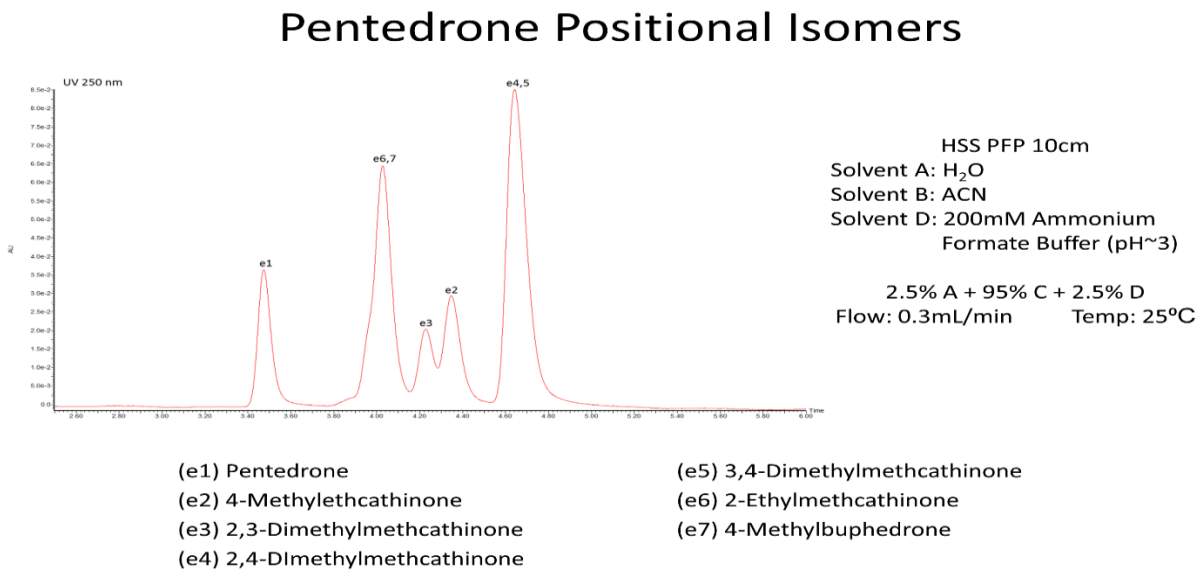

Figure 14- UHPLC separation of pentedrone positional isomers employing a PFP column in the HILIC mode.

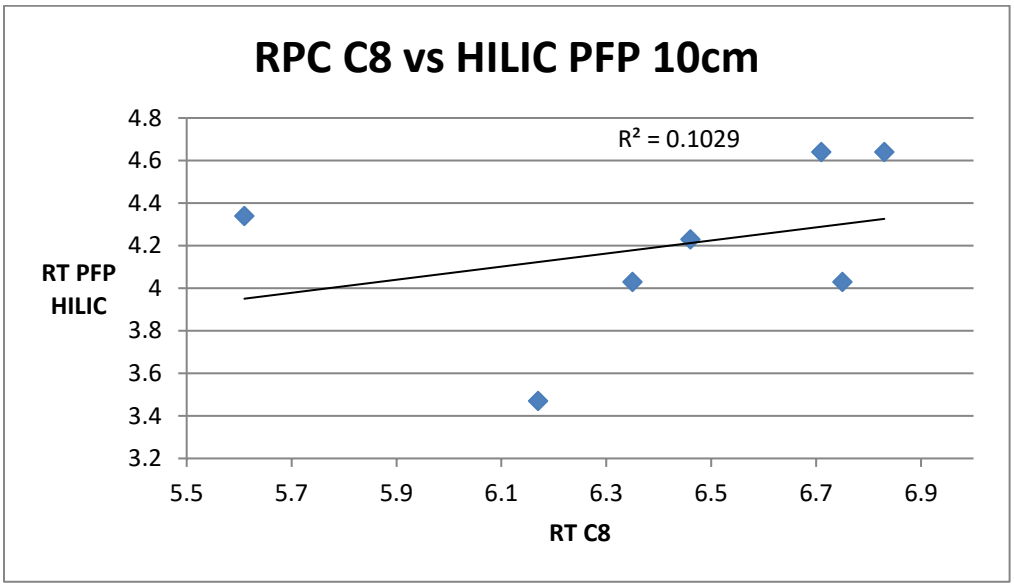

Figure 15- RT C8 versus RT PFP for a mixture of pentedrone positional isomers.

This resource was prepared by the author(s) using Federal funds provided by the U.S. Department of Justice. Opinions or points of view expressed are those of the author(s) and do not necessarily reflect the official position or policies of the U.S. Department of Justice.

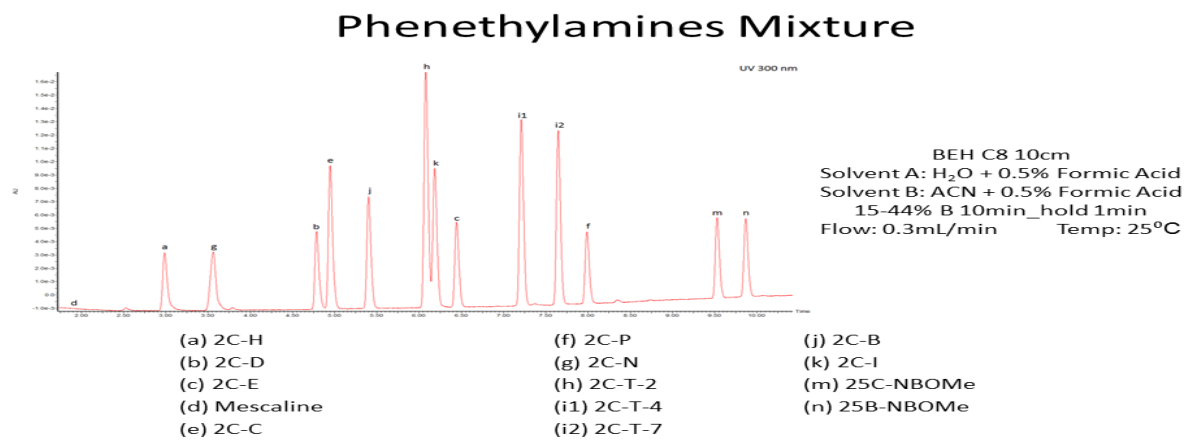

Figure 16- UHPLC separation of controlled phenethylamines employing a C8 column.

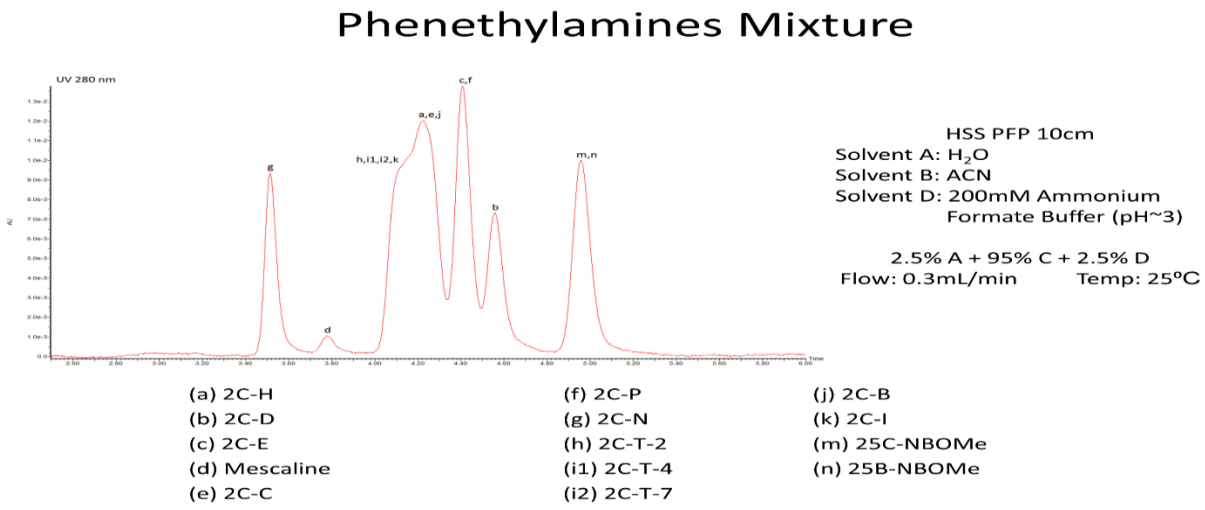

Figure 17- UHPLC separation of controlled phenethylamines employing a PFP column in the HILIC mode.

This resource was prepared by the author(s) using Federal funds provided by the U.S. Department of Justice. Opinions or points of view expressed are those of the author(s) and do not necessarily reflect the official position or policies of the U.S. Department of Justice.

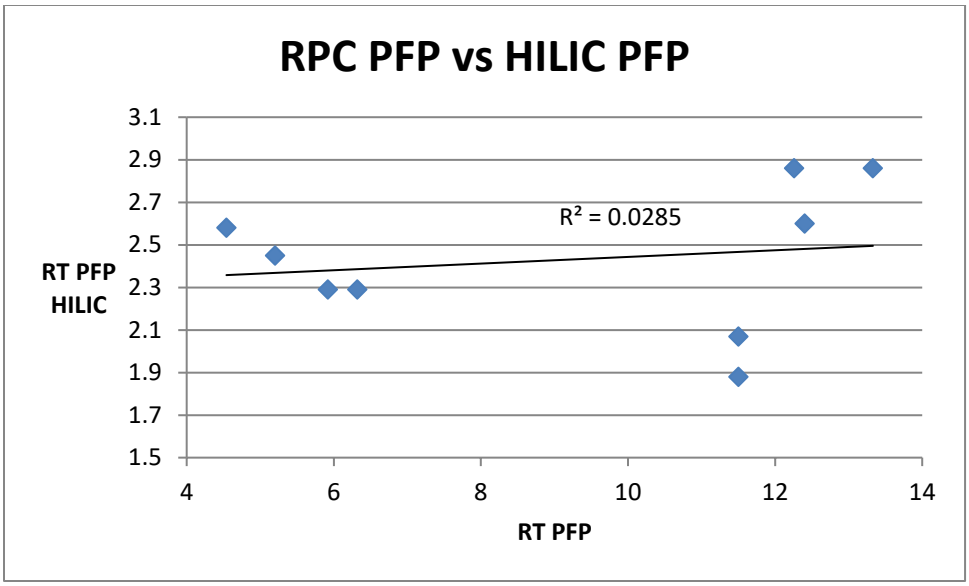

Figure 18- RT C8 versus RT PFP for a mixture of controlled synthetic phenethylamines.

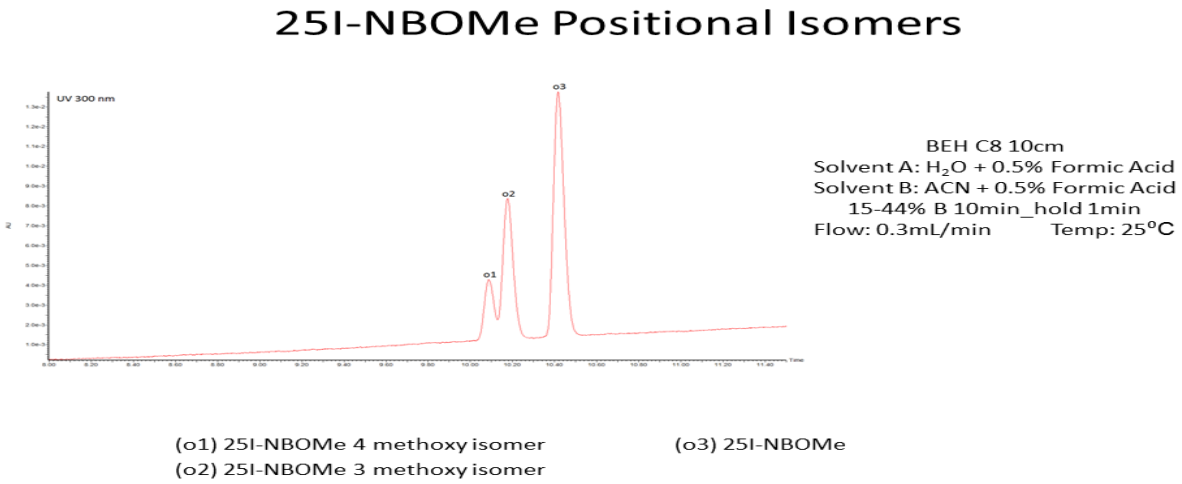

Figure 19- UHPLC separation of 25I-NBOMe positional isomers employing a C8 column.

This resource was prepared by the author(s) using Federal funds provided by the U.S. Department of Justice. Opinions or points of view expressed are those of the author(s) and do not necessarily reflect the official position or policies of the U.S. Department of Justice.

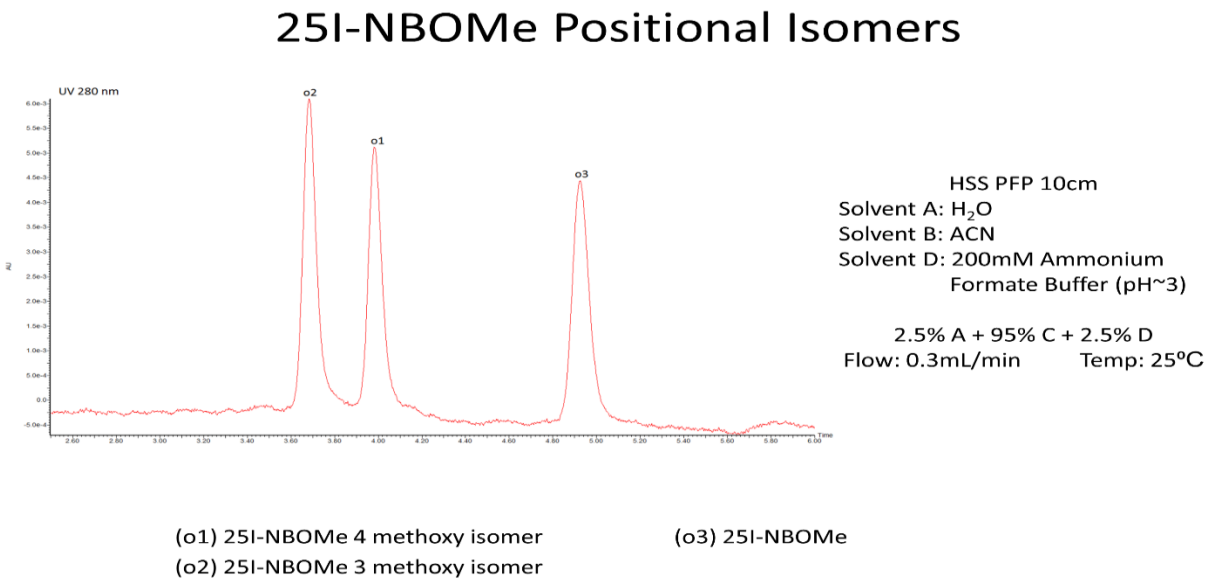

Figure 20- UHPLC separation of 25I-NBOMe positional isomers employing a PFP column in the HILIC mode.

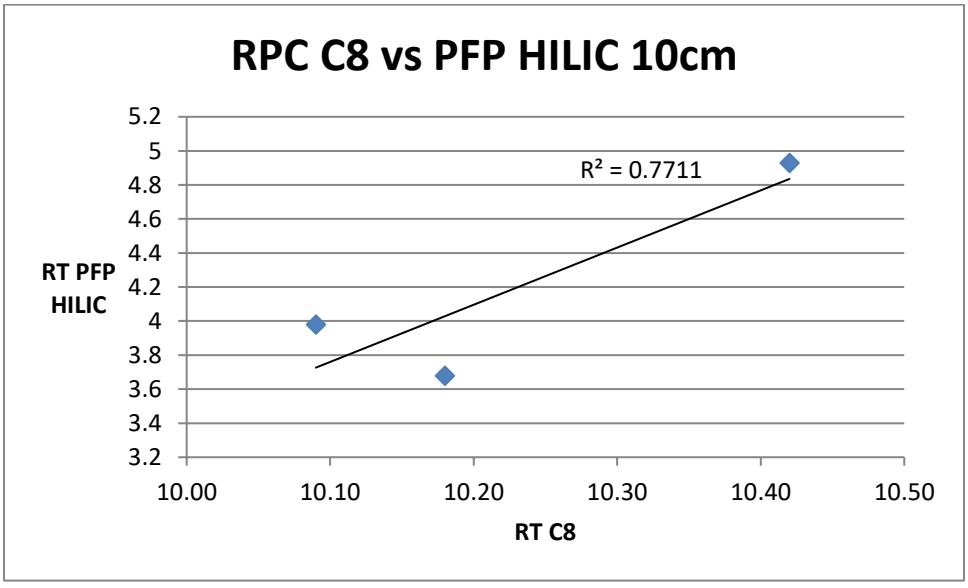

Figure 21- RT C8 versus RT PFP for a mixture of phenethylamine 25I isomers.

This resource was prepared by the author(s) using Federal funds provided by the U.S. Department of Justice. Opinions or points of view expressed are those of the author(s) and do not necessarily reflect the official position or policies of the U.S. Department of Justice.

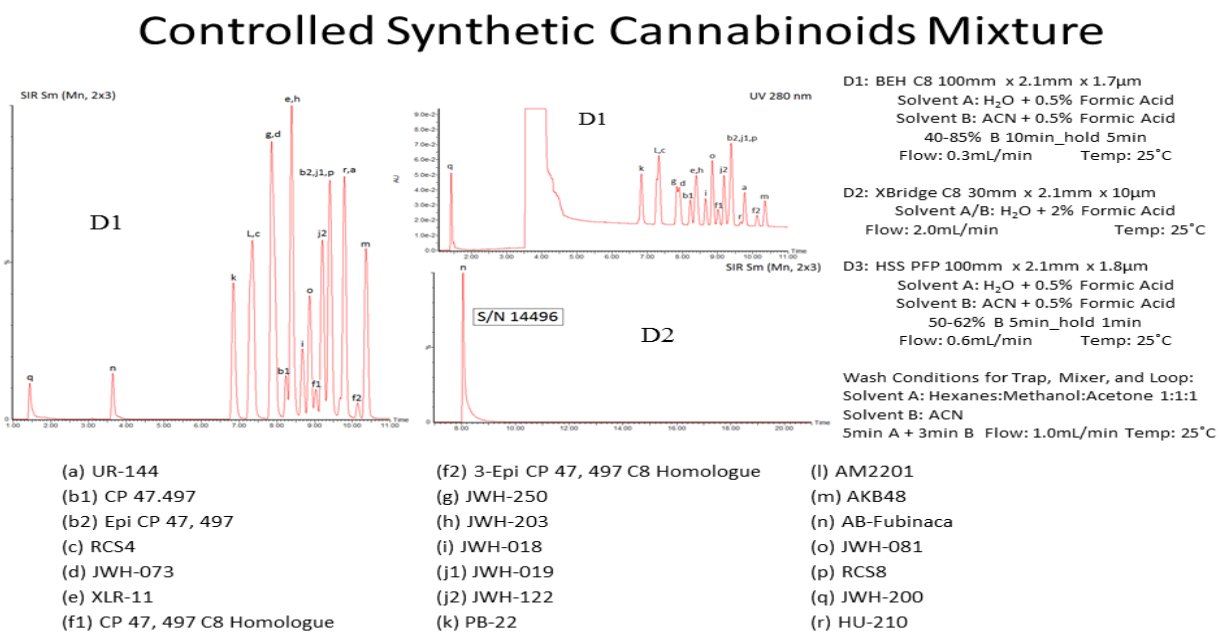

Figure 22- Multi-dimensional separation of a selected controlled synthetic cannabinoid.

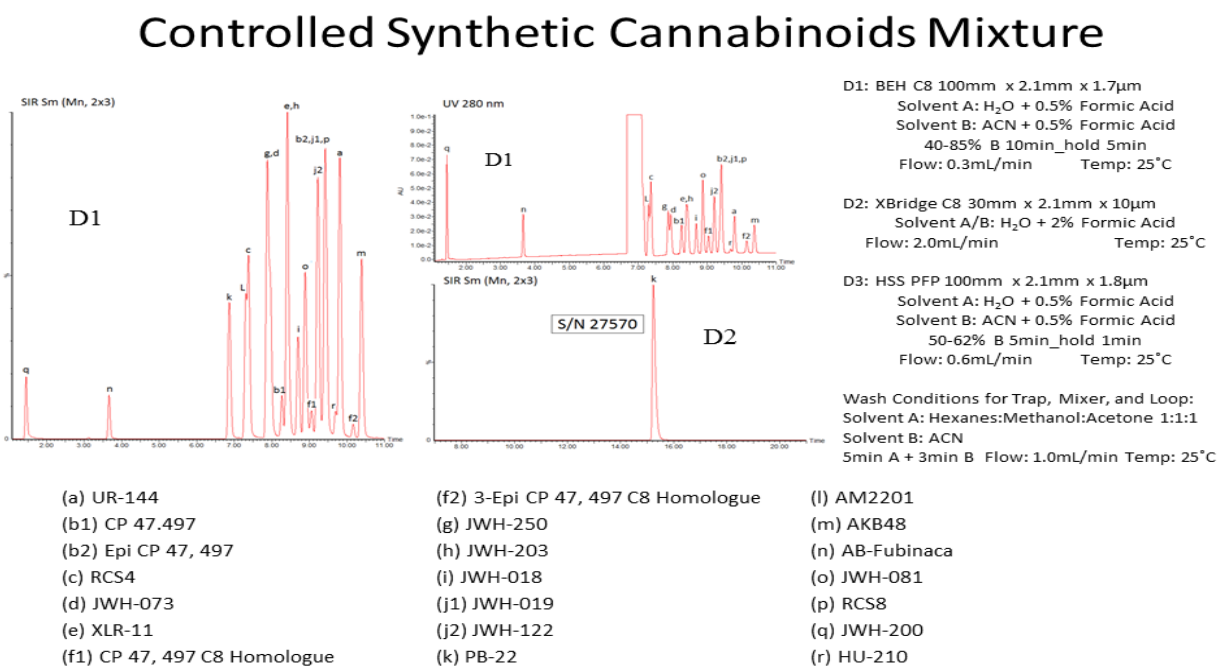

Figure 23- Multi-dimensional separation of a selected controlled synthetic cannabinoid.

This resource was prepared by the author(s) using Federal funds provided by the U.S. Department of Justice. Opinions or points of view expressed are those of the author(s) and do not necessarily reflect the official position or policies of the U.S. Department of Justice.

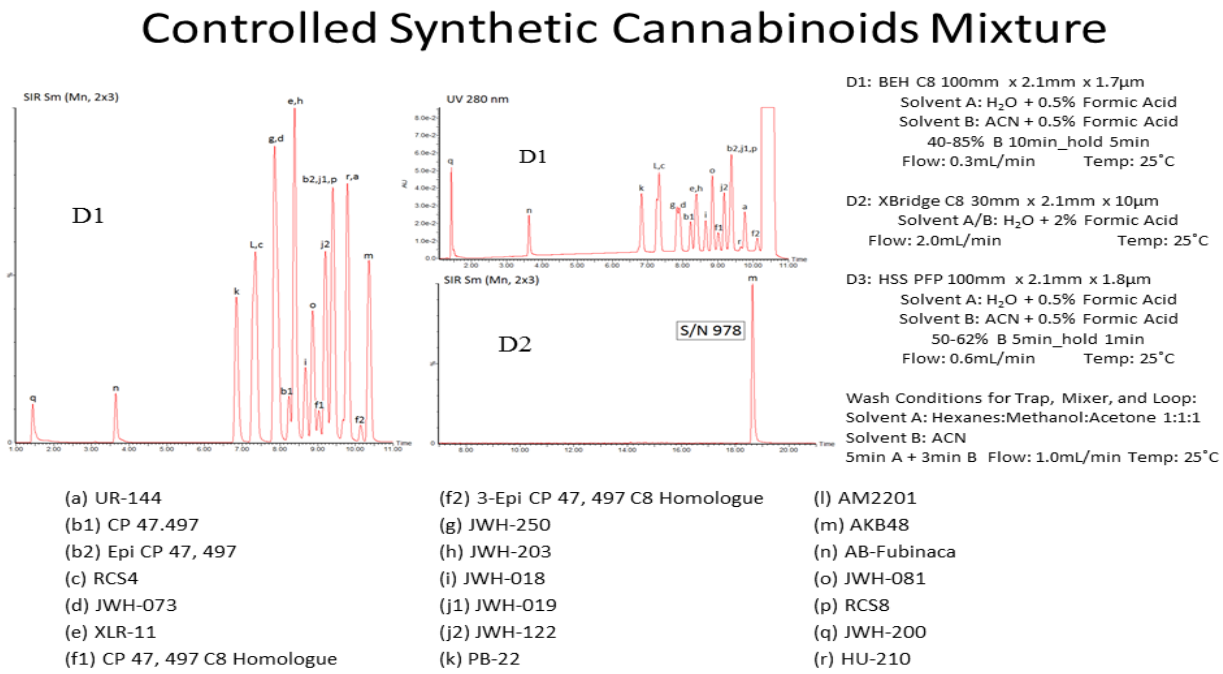

Figure 24- Multi-dimensional separation of a selected controlled synthetic cannabinoid.

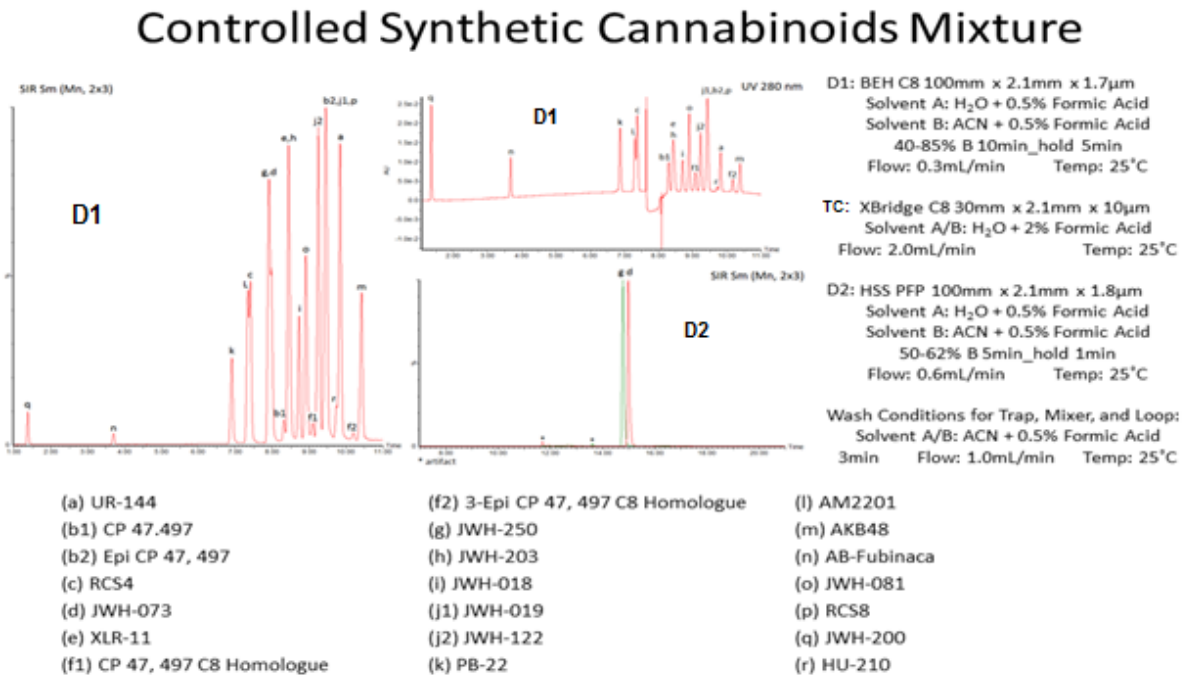

Figure 25- Multi-dimensional separation of selected controlled synthetic cannabinoids co-eluting in the first separation dimension.

This resource was prepared by the author(s) using Federal funds provided by the U.S. Department of Justice. Opinions or points of view expressed are those of the author(s) and do not necessarily reflect the official position or policies of the U.S. Department of Justice.

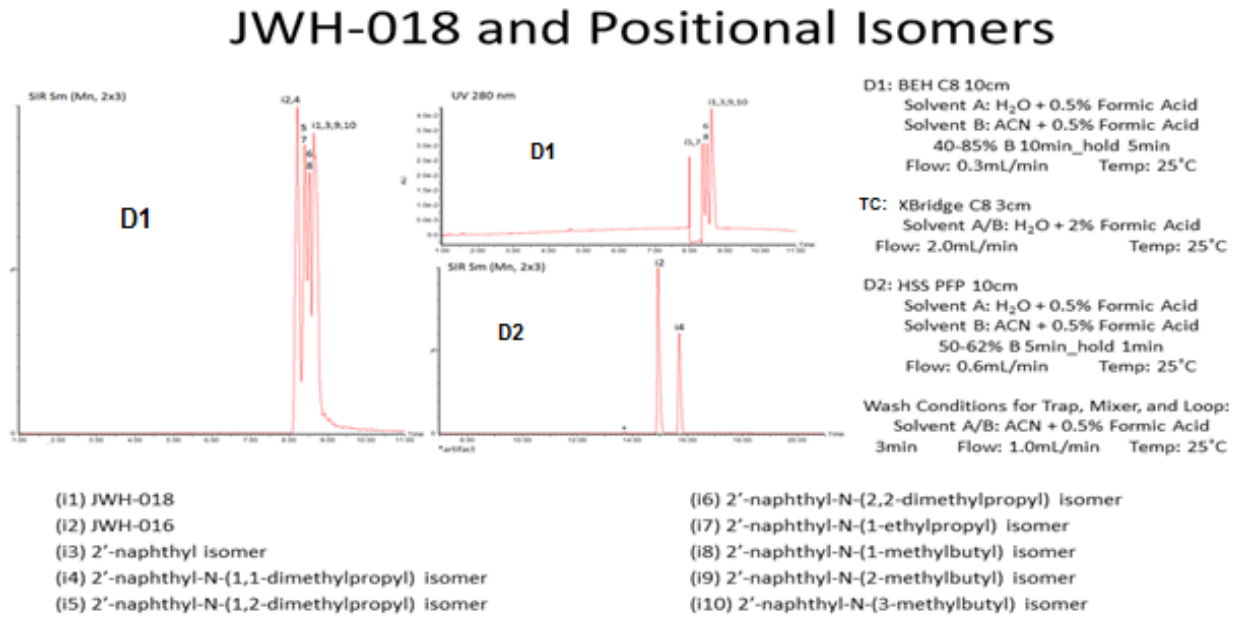

Figure 26- Multi-dimensional separation of selected JWH-018 positional isomers co-eluting in the first separation dimension.

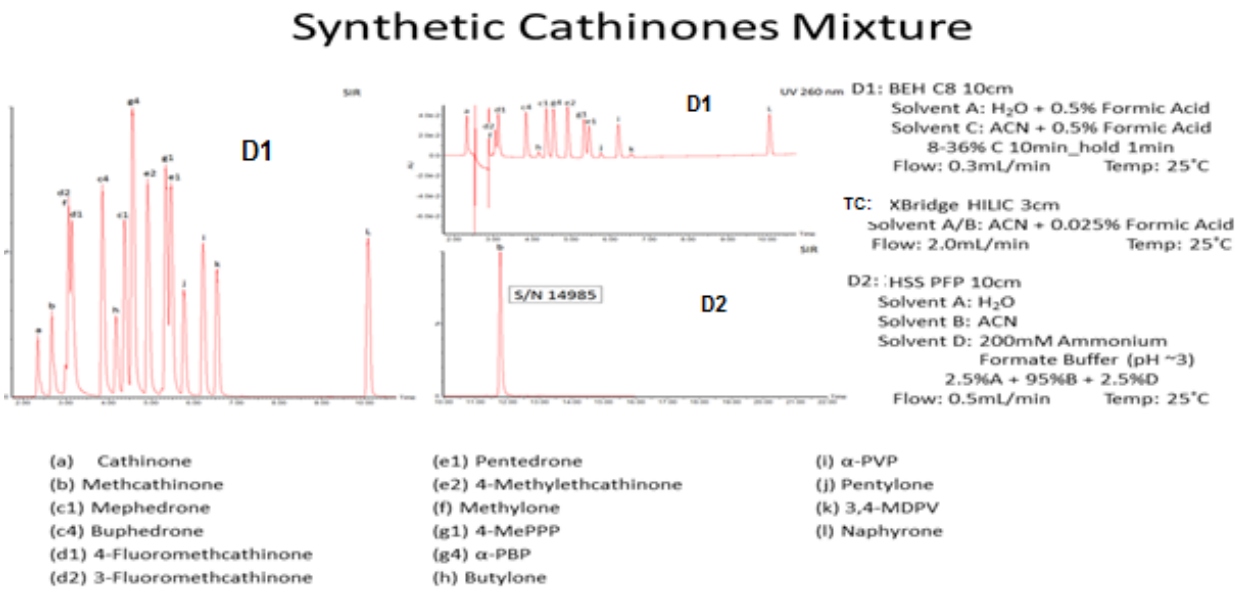

Figure 27- Multi-dimensional separation of a selected controlled synthetic cathinone.

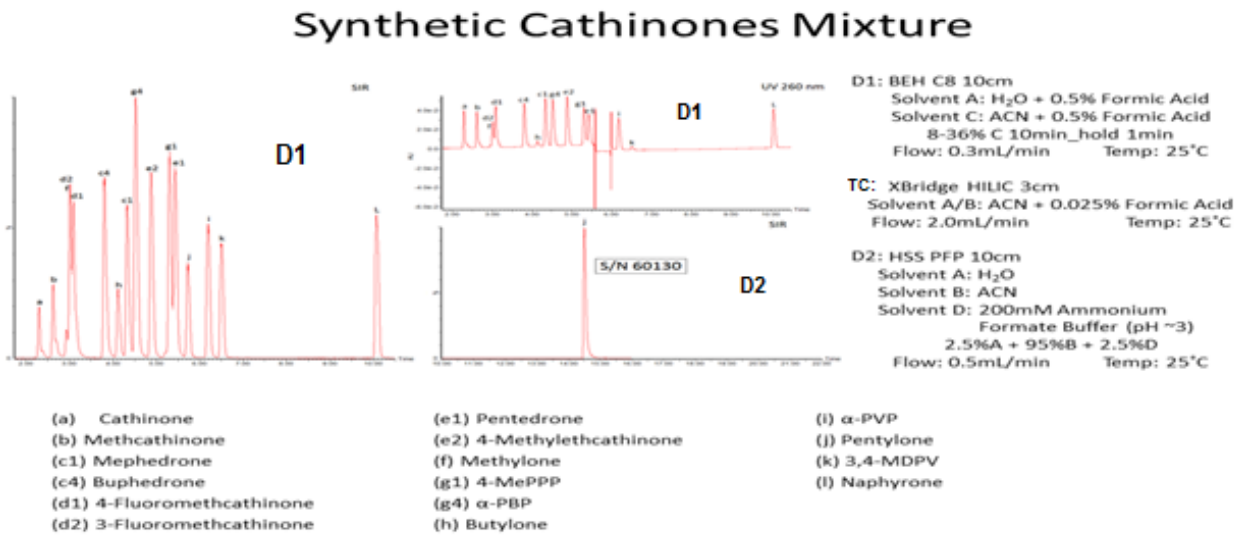

Figure 28- Multi-dimensional separation of a selected controlled synthetic cathinone.

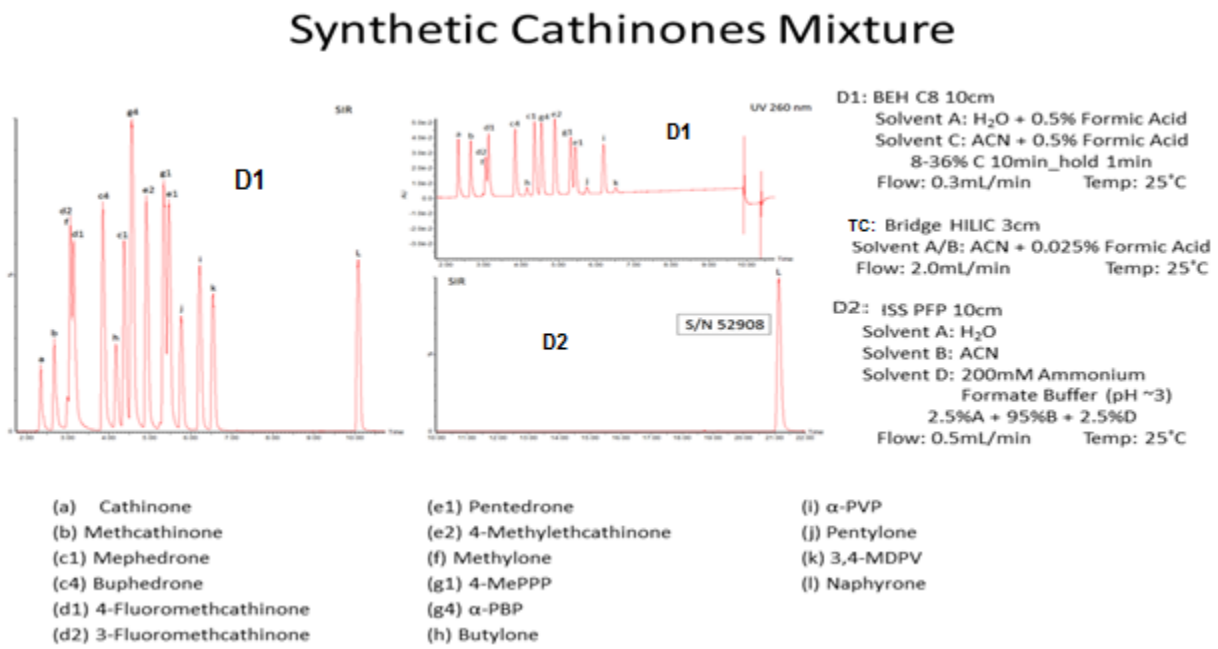

Figure 29- Multi-dimensional separation of a selected controlled synthetic cathinone.

This resource was prepared by the author(s) using Federal funds provided by the U.S. Department of Justice. Opinions or points of view expressed are those of the author(s) and do not necessarily reflect the official position or policies of the U.S. Department of Justice.

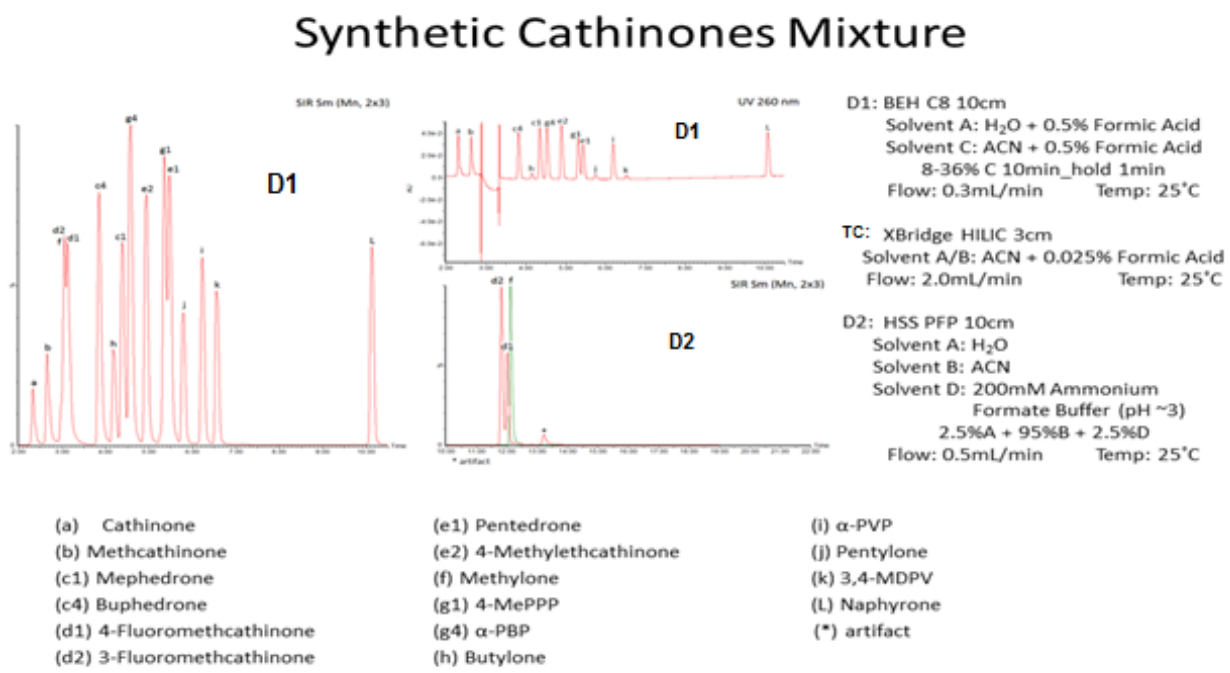

Figure 30- Multi-dimensional separation of selected synthetic cathinones co-eluting in the first separation dimension.

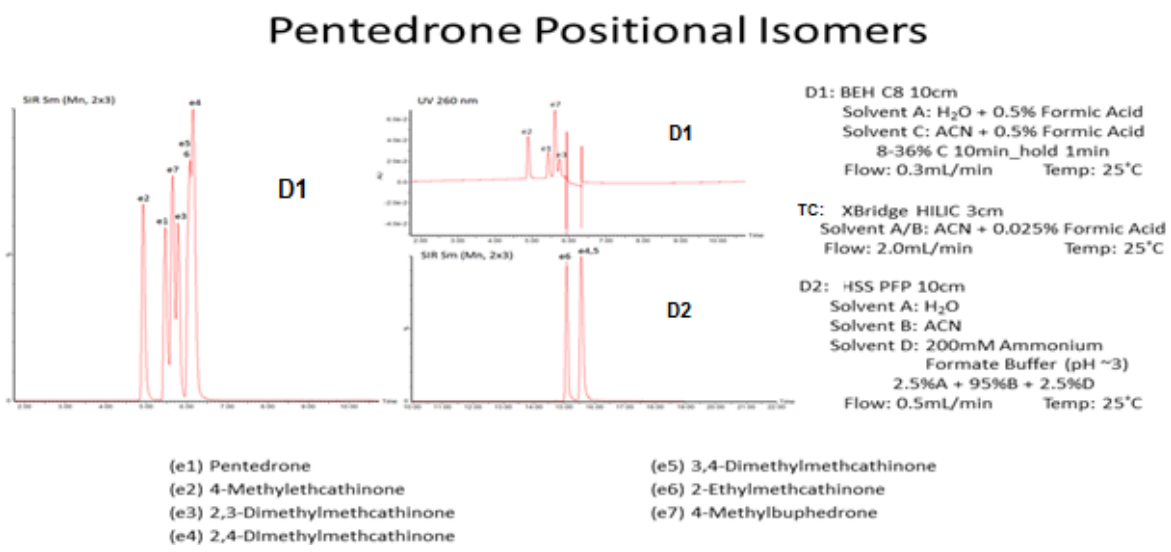

Figure 31- Multi-dimensional separation of selected pentedrone positional isomers co-eluting in the first separation dimension.

This resource was prepared by the author(s) using Federal funds provided by the U.S. Department of Justice. Opinions or points of view expressed are those of the author(s) and do not necessarily reflect the official position or policies of the U.S. Department of Justice.

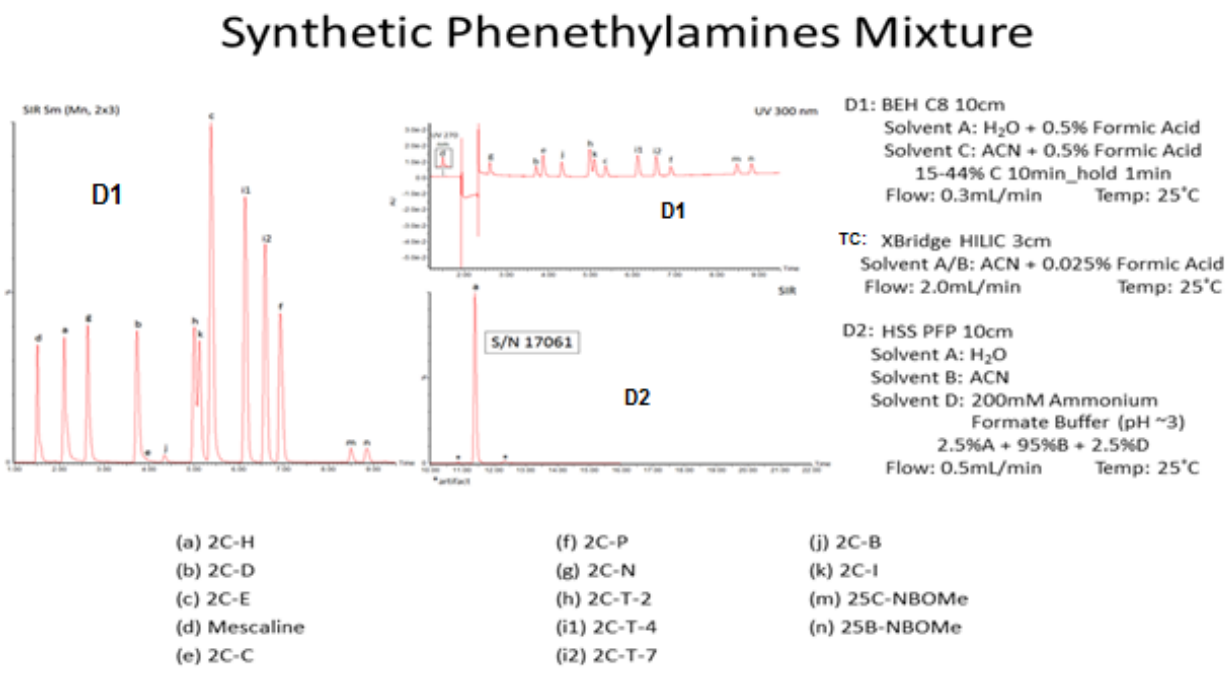

Figure 32- Multi-dimensional separation of a selected controlled phenethylamine.

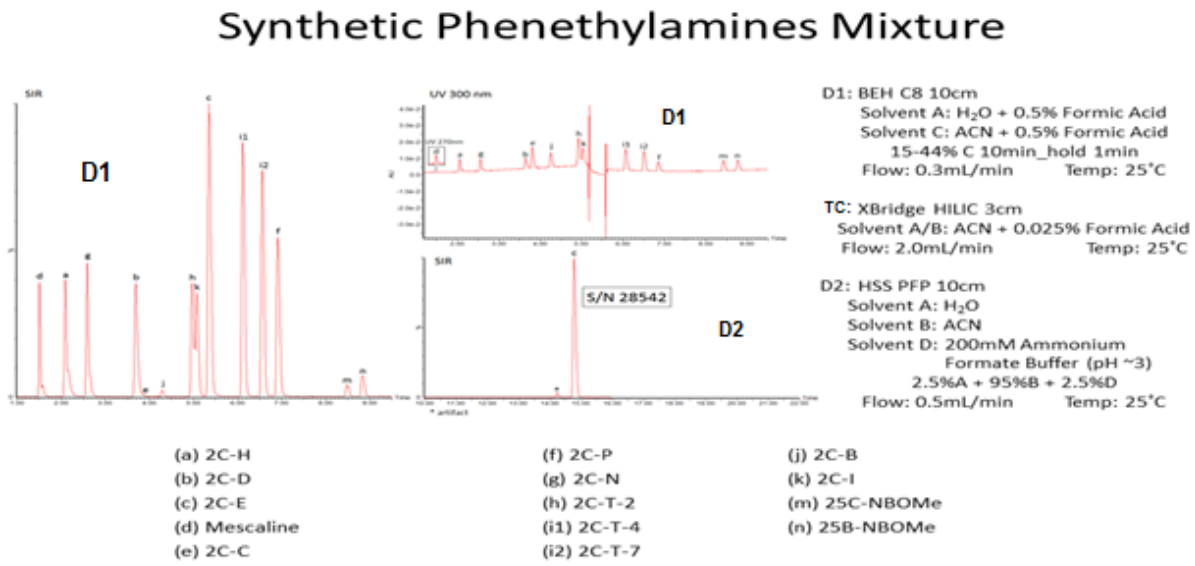

Figure 33- Multi-dimensional separation of a selected controlled phenethylamine.

This resource was prepared by the author(s) using Federal funds provided by the U.S. Department of Justice. Opinions or points of view expressed are those of the author(s) and do not necessarily reflect the official position or policies of the U.S. Department of Justice.

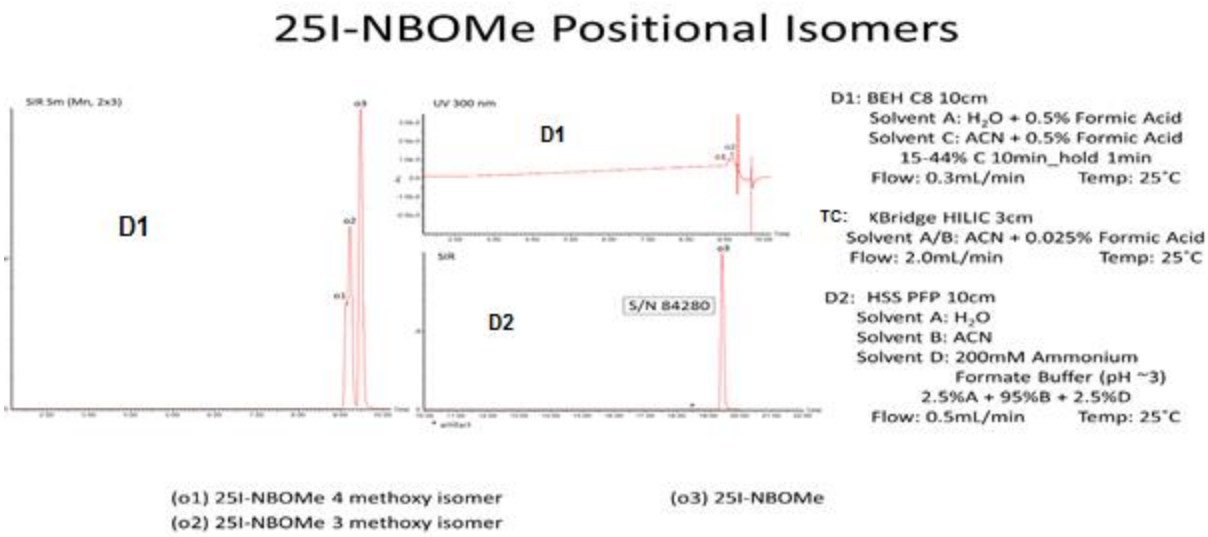

Figure 34- Multi-dimensional separation of a selected 25I-NBOMe positional isomer.

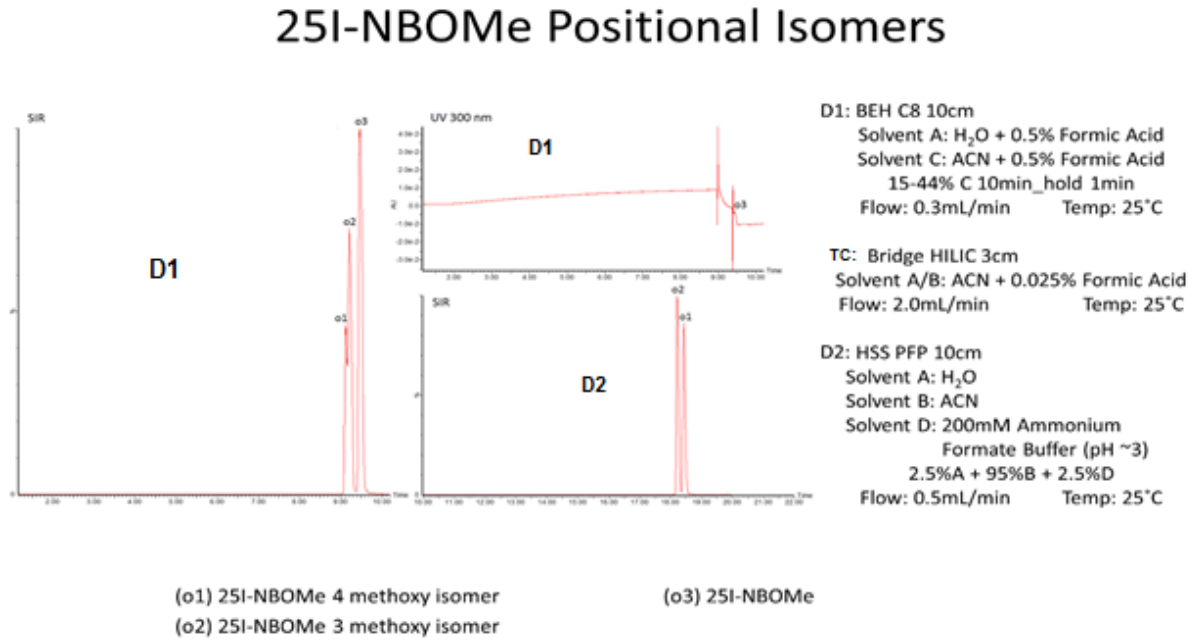

Figure 35- Multi-dimensional separation of selected 25I-NBOMe positional isomers co-eluting in the first separation dimension.

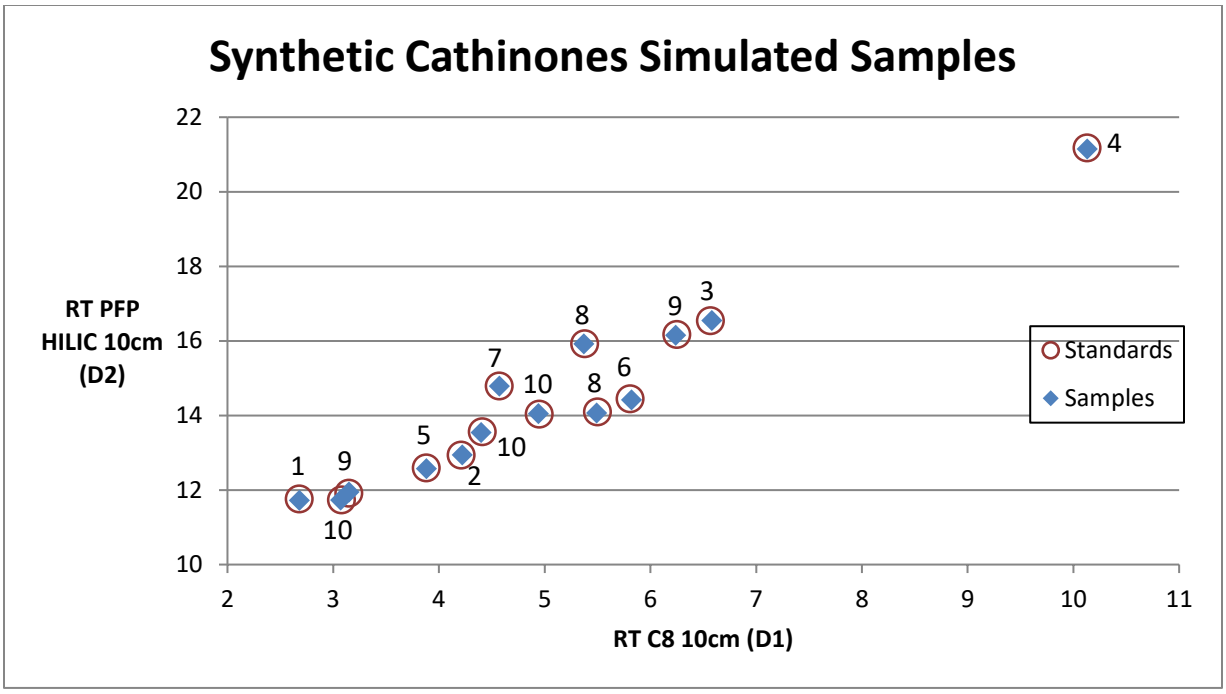

Figure 36- Multi-dimensional analysis of simulated synthetic cathinone samples described in Table 5.

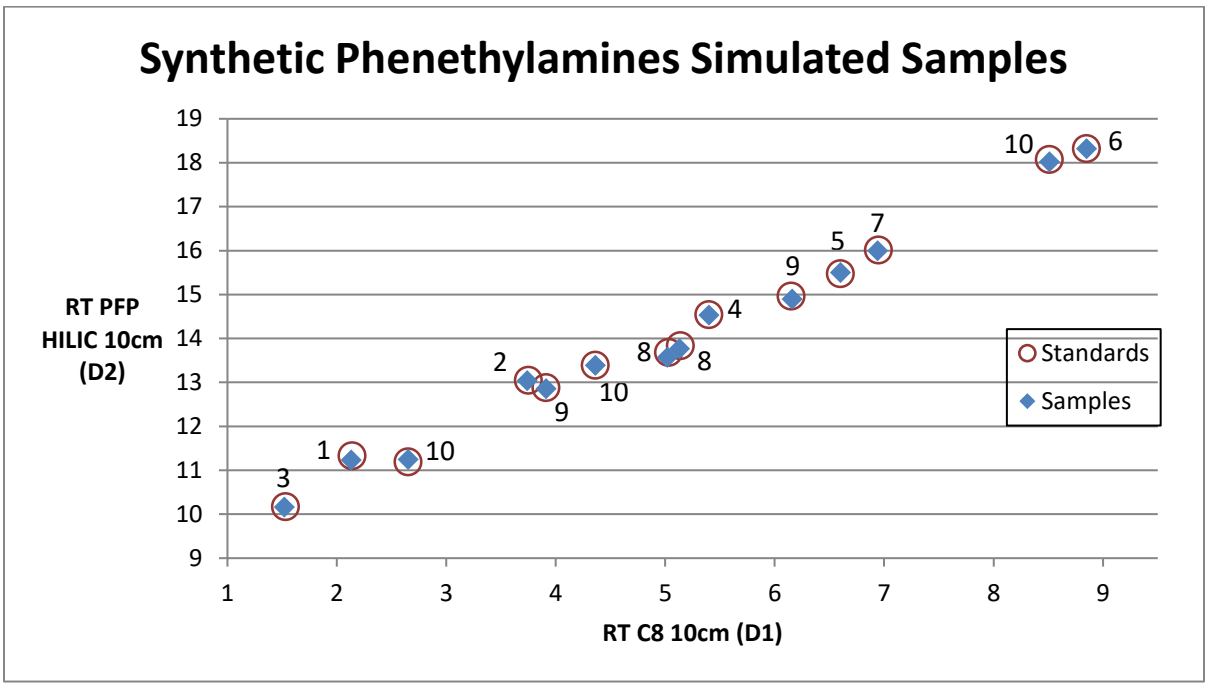

Figure 37- Multi-dimensional analysis of simulated phenethylamine samples described in Table 6.

This resource was prepared by the author(s) using Federal funds provided by the U.S. Department of Justice. Opinions or points of view expressed are those of the author(s) and do not necessarily reflect the official position or policies of the U.S. Department of Justice.

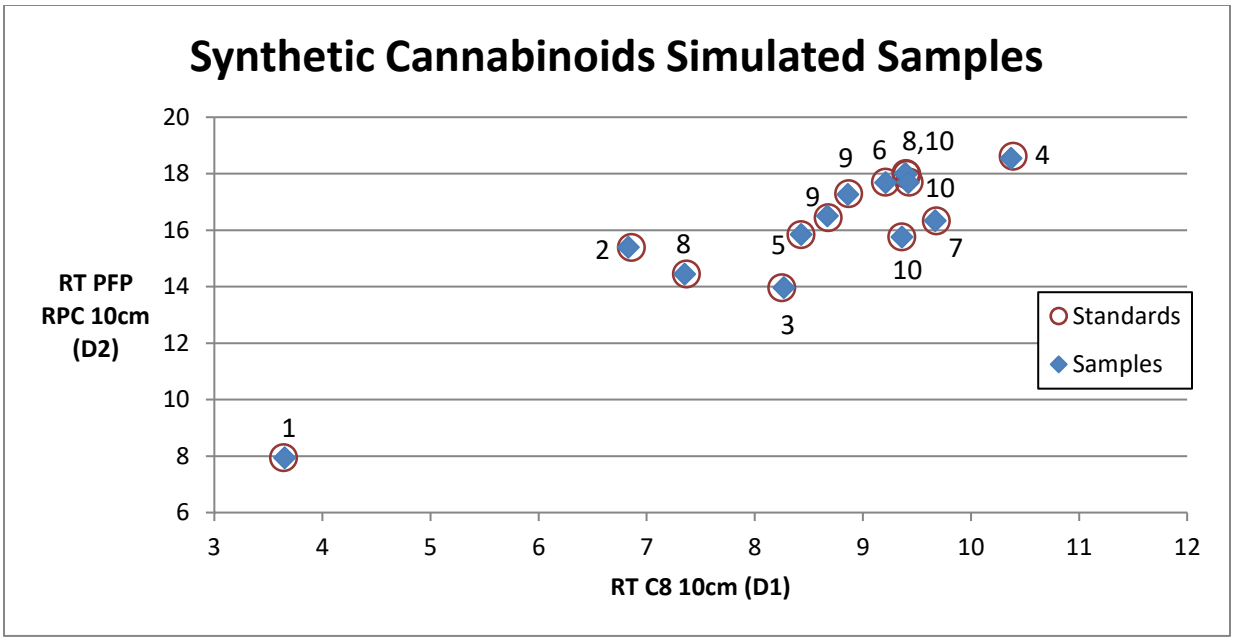

Figure 38- Multi-dimensional analysis of simulated synthetic cannabinoid samples described in Table 7.

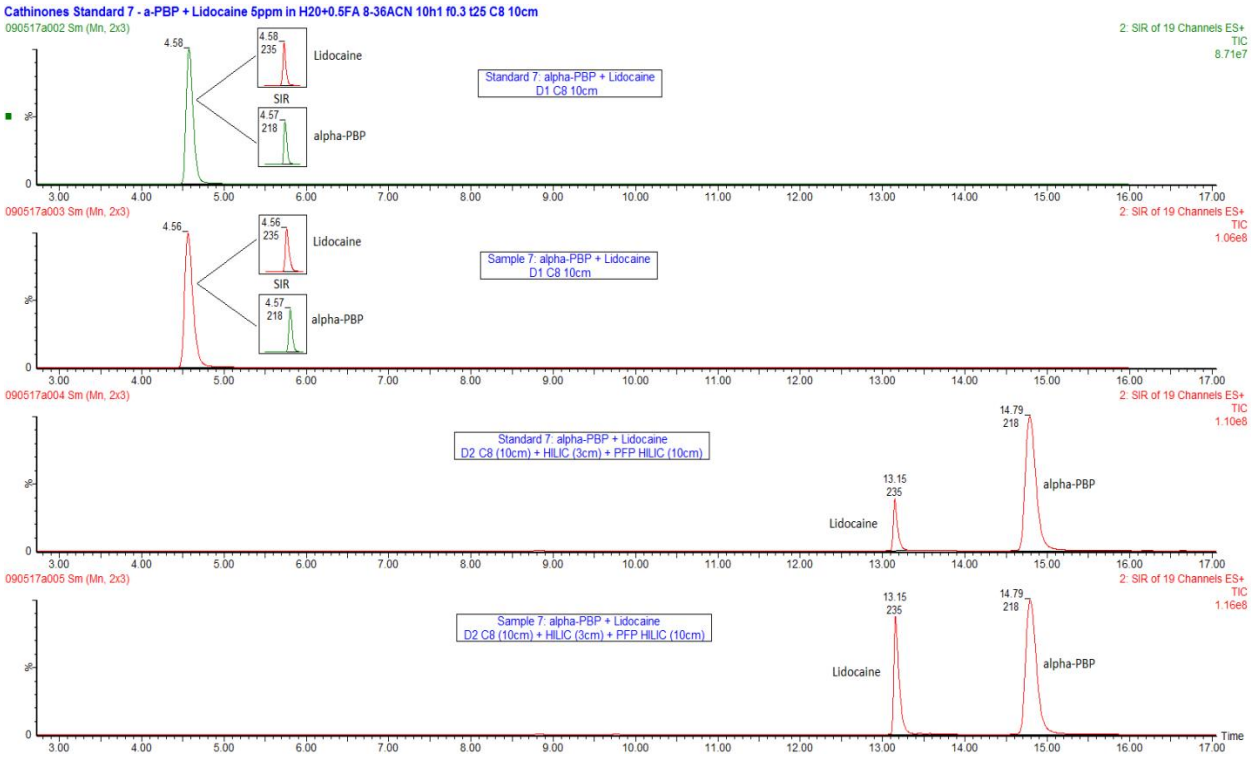

Figure 39- Multi-dimensional analysis of simulated synthetic cathinone sample 7 described in Table 5.

This resource was prepared by the author(s) using Federal funds provided by the U.S. Department of Justice. Opinions or points of view expressed are those of the author(s) and do not necessarily reflect the official position or policies of the U.S. Department of Justice.

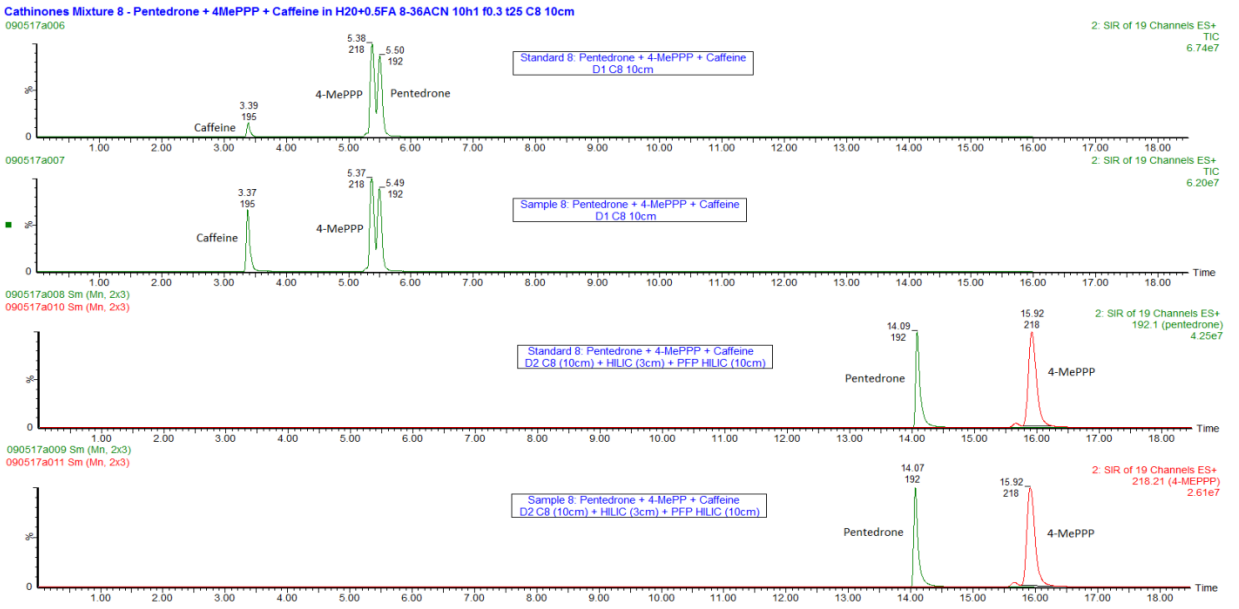

Figure 40- Multi-dimensional analysis of simulated synthetic cathinone sample 8 described in Table 5.

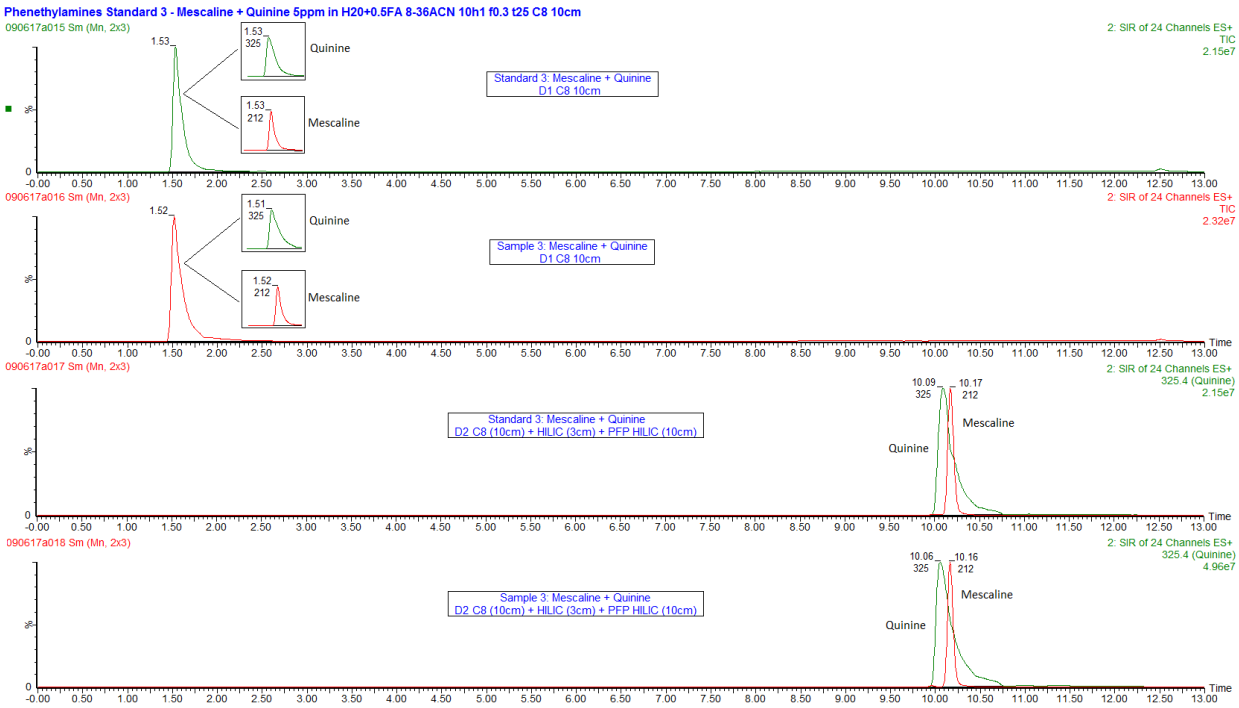

Figure 41- Multi-dimensional analysis of simulated phenethylamine sample 3 described in Table 6.

This resource was prepared by the author(s) using Federal funds provided by the U.S. Department of Justice. Opinions or points of view expressed are those of the author(s) and do not necessarily reflect the official position or policies of the U.S. Department of Justice.

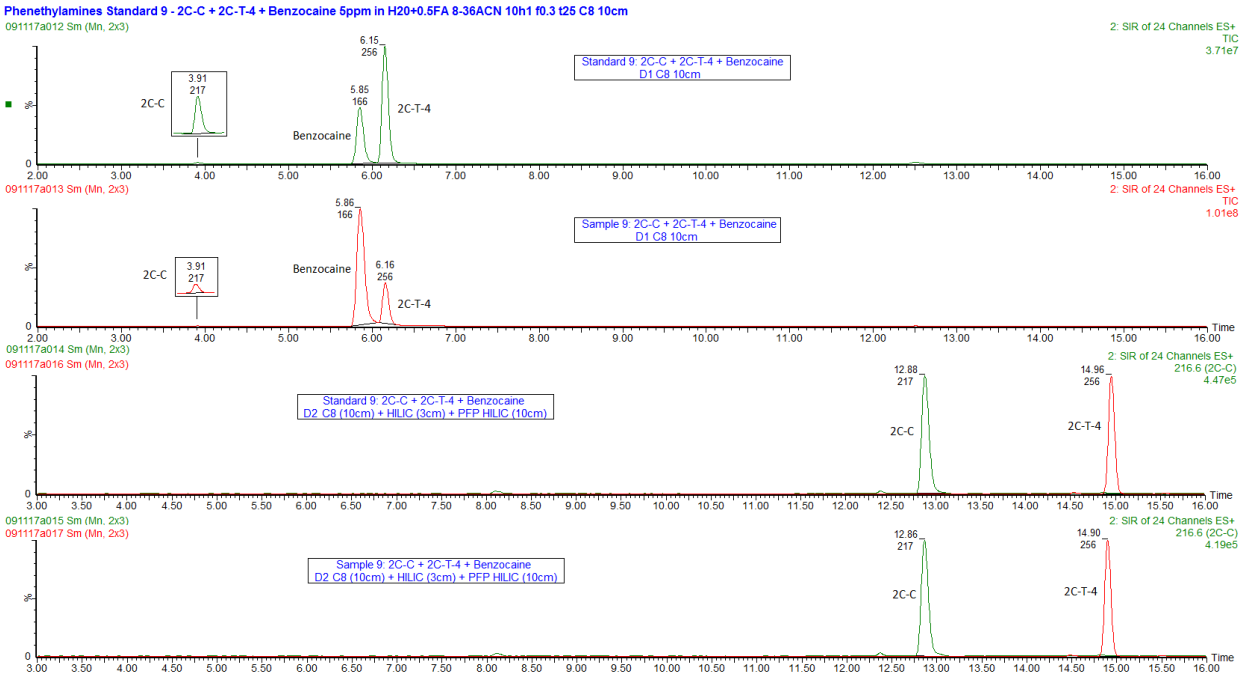

Figure 42- Multi-dimensional analysis of simulated phenethylamine sample 9 described in Table 6.

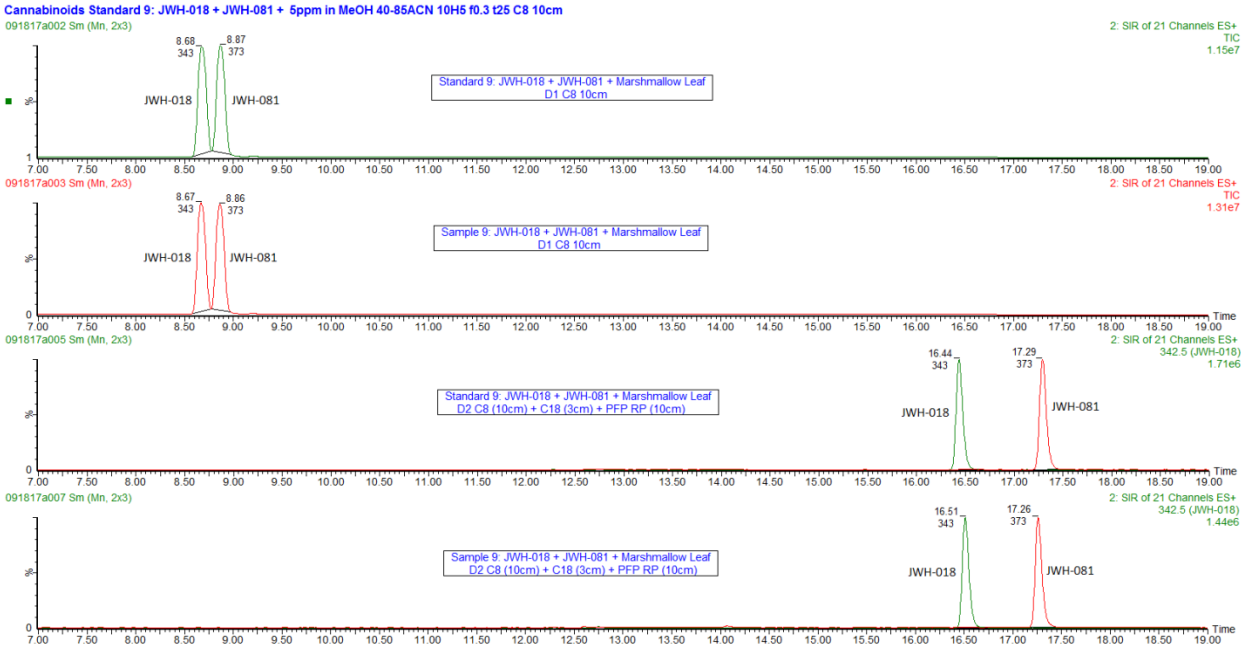

Figure 43- Multi-dimensional analysis of simulated synthetic cannabinoid sample 9 described in Table 7.

This resource was prepared by the author(s) using Federal funds provided by the U.S. Department of Justice. Opinions or points of view expressed are those of the author(s) and do not necessarily reflect the official position or policies of the U.S. Department of Justice.

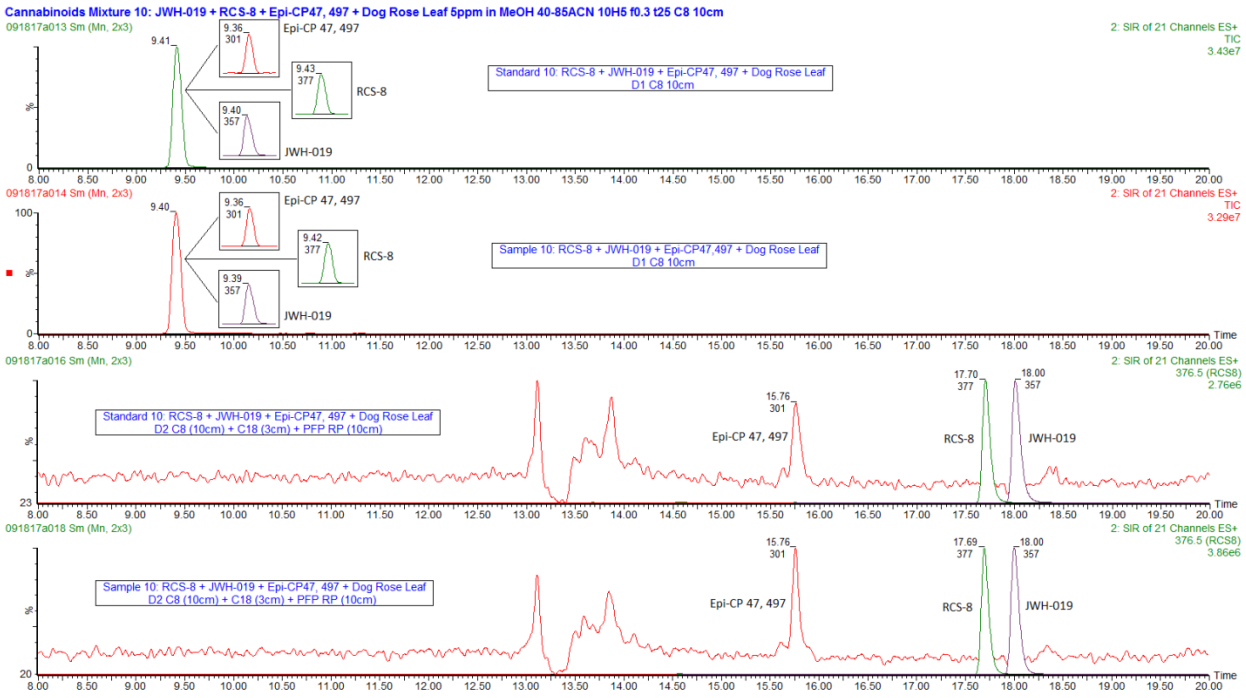

Figure 44- Multi-dimensional analysis of simulated synthetic cannabinoid sample 10 described in Table 7.